

TECHNICAL REPORT #36

Smithsonian Institution &
The University of Arizona*

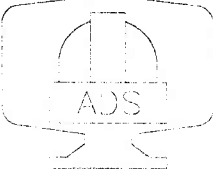

Secondary Mirrors Support:

M2/F5 Hexapod Design Technical Report

& M2/F5 Hexapod Test Report

ADS International s.r.l.

May 2001

	MMT CONVERSION	 Steward Observatory
	Doc.No. : H5-RP-AD-99001 Issue : E Date : 17 May 2000	

MMT CONVERSION

SECONDARY MIRRORS SUPPORT

M2/F5 HEXAPOD DESIGN TECHNICAL REPORT

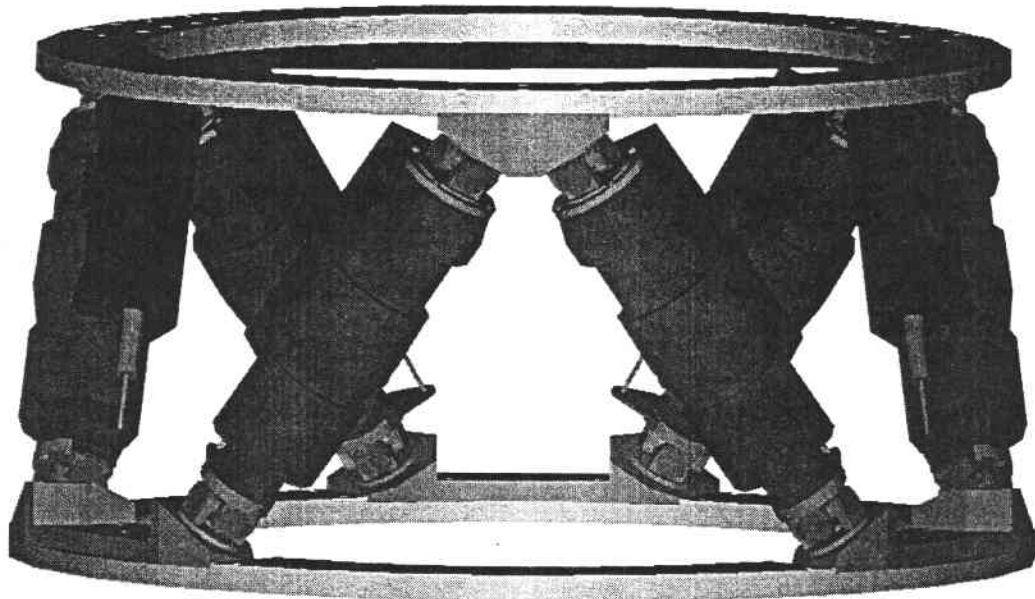
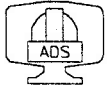



TABLE OF CONTENTS

1. INTRODUCTION	4
2. HEXAPOD ORIENTATION	5
3. KINEMATIC ANALYSIS	6
4. JOINTS DESIGN	9
5. MECHANICAL DESIGN	11
5.1 – Actuator stiffness	13
6. FINITE ELEMENTS ANALYSIS	14
6.1 – Static Analysis	15
6.2 – Modal Analysis	16
7. FINAL REMARKS	19
ANNEX 1	20

	MMT CONVERSION	Doc.No: H5-RP-AD-99001 Issue : E Date : 17 May 2000	
---	-----------------------	---	---

APPLICABLE DOCUMENTS AND REFERENCES

1. Statement of Work (SOW), "The f/5 hexapod positioning system for the MMT Conversion Project", March 2nd 1999;
2. W.Gallieni, R.Pozzi; "MMT Conversion – Secondary Mirrors Support – M2/f15 and M2/f9 Hexapod Design – Technical Report", Issue 3, January 1997;
3. E-mail by S. West dated 7-Feb.-2000.

	MMT CONVERSION	Doc.No: H5-RP-AD-99001 Issue : E Date : 17 May 2000	
--	-----------------------	---	--

1. INTRODUCTION

This document reports on the design of the hexapod supporting the $f/5$ secondary mirror.

The hexapod is designed accounting for the constraints given by the existing M2 hub and the mirror unit itself (ref. 1).

Hexapod static and dynamic analysis are studied by modelling the whole M2 hub in the $f/5$ configuration.

The $f/9$ - $f/15$ hexapod design (ref. 2) is assumed as baseline for the $f/5$ development.

2. HEXAPOD ORIENTATION

The hexapod layout is sketched in figure 1. The gravity vector shows the hexapod orientation with respect to the telescope elevation axis.

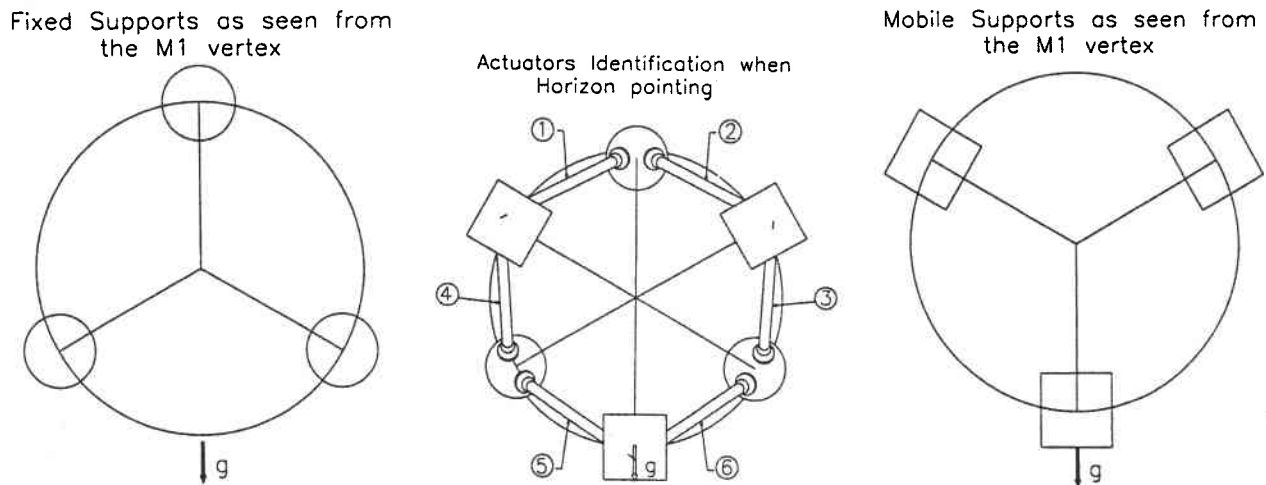


Figure 1. Hexapod orientation.

This orientation has been selected to minimise the difference between the forces in the actuators at different telescope elevations. The reverse one (with gravity upward in figure 1) leads to almost similar forces, while the 90 deg. rotated ones must be avoided.

The hexapod layout is specified to have the mirror c.o.g. placed onto the plane defined by the intersection of the six actuator axis (three pairs).

Moreover, the six hexapod axes should appear aligned on a triangle, when observed on the plan view of the hexapod wireframe (ref. 1).



3. KINEMATIC ANALYSIS

The kinematic model assumes the actuator length being the distance between the axis of its two joints, that is the kinematic joints is lumped on its center.

The mobile and fixed plates are defined by the kinematic joints plane.

The center of rotation is the mirror vertex. The mirror c.o.g. is centred on the plane defined by the actuators axis intersection, as specified by ref.1 – 3.2.2 .

The hexapod specifications (ref. 1) relevant to the kinematic design are hereafter reported:

- $Z = \pm 12 \text{ mm};$
- $X, Y = \pm 17 \text{ mm};$
- $TILT_{X,Y} = \pm 1.2 \text{ deg.}$

The kinematic model parameters are derived from the wireframe of hexapod layout.

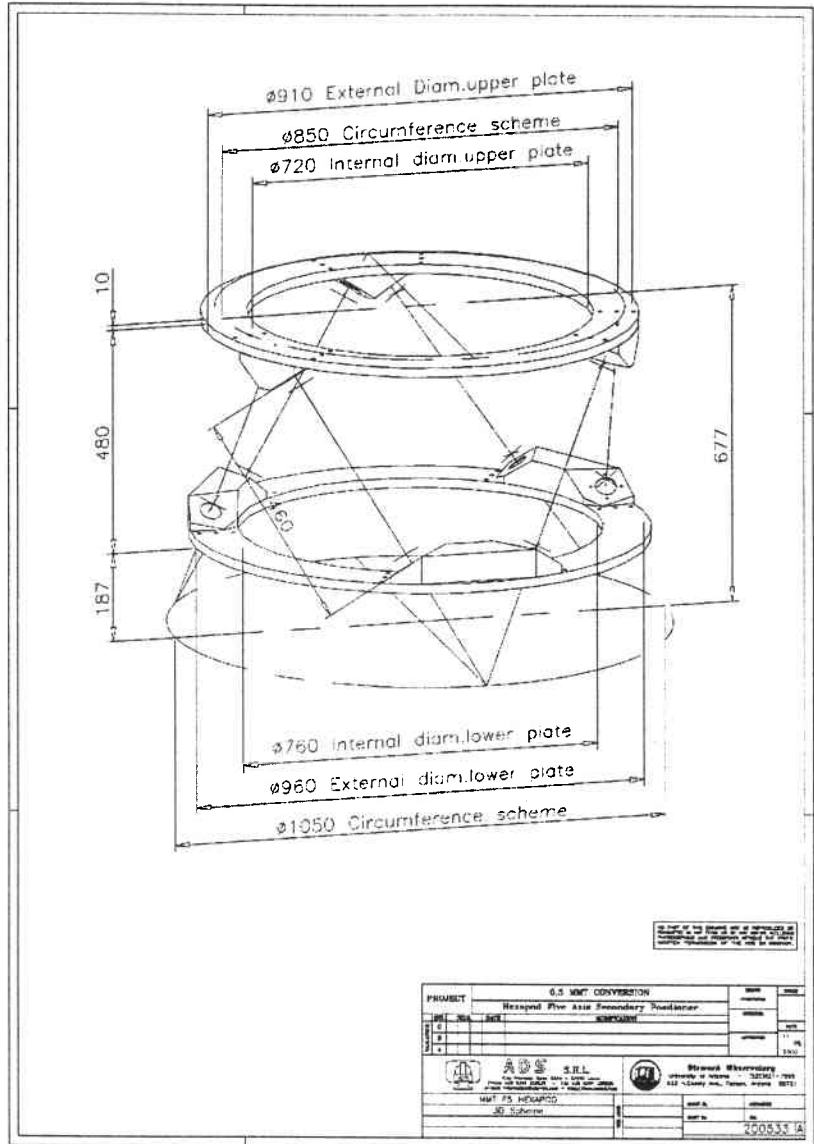


Figure 2. Hexapod wireframe.

Actuator nominal length (measured between the centres of the two joints):	$L_0 = 413 \text{ mm}$
Mobile plate joints minimum distance:	$D_{\text{MOB}} = 281.06 \text{ mm}$
Fixed plate joints minimum distance:	$D_{\text{FIX}} = 110.50 \text{ mm}$
Distance between the center of rotation (mirror vertex) and the centre of the mobile platform (mobile joints plane):	$H = 365 + 71.5 = 436.5 \text{ mm}$

The maximum actuator stroke is $\pm 25 \text{ mm}$. The limit switches are placed at $\pm 23 \text{ mm}$ and the mechanical stops (TBD) at $\pm 24 \text{ mm}$. The joints max allowed and combined rotation is $\pm 6 \text{ deg}$.

The results of the kinematic analysis are reported in table1.

TASK	$\Delta Z \text{ (mm)}$	$\Delta X, \Delta Y \text{ (mm)}$	$\Delta \theta \text{ (deg)}$	$\Delta L_{\text{ACT}} \text{ (mm)}$	$\Delta \theta_{\text{JOINTS}} \text{ (deg)}$
Focus	37	0	0	23	1.5
Lateral offset	0	30	0	23	5
Tip-Tilt	0	0	3.5	23	5
COMBINED	12	9	1.2	23	3.1

Table 1. Kinematic analysis results.

Figure 3 shows the actuators elongation for the manoeuvre given by the following sequence:

- displace the mobile plate center by $X=9\text{mm}$, $Y=9\text{mm}$ and $Z=12\text{mm}$;
- rotate the mobile plate by 1.2 deg around the mirror vertex;
- perform with the mobile plate the complete 360 deg rotation around the fixed plate Z axis.

Figure 4 reports the universal joints rotations during the same manoeuvre.

The kinematic analysis shows that the HP largely fulfils the individual stroke requirements.

For what concerns the worst case simultaneous combination of the specified motion the 23 mm actuator stroke limits the shift and tilt envelope.

Such limitation is automatically provided by the end stroke limit switches implemented into each actuator and then by the mechanical stops inside the actuators themselves.

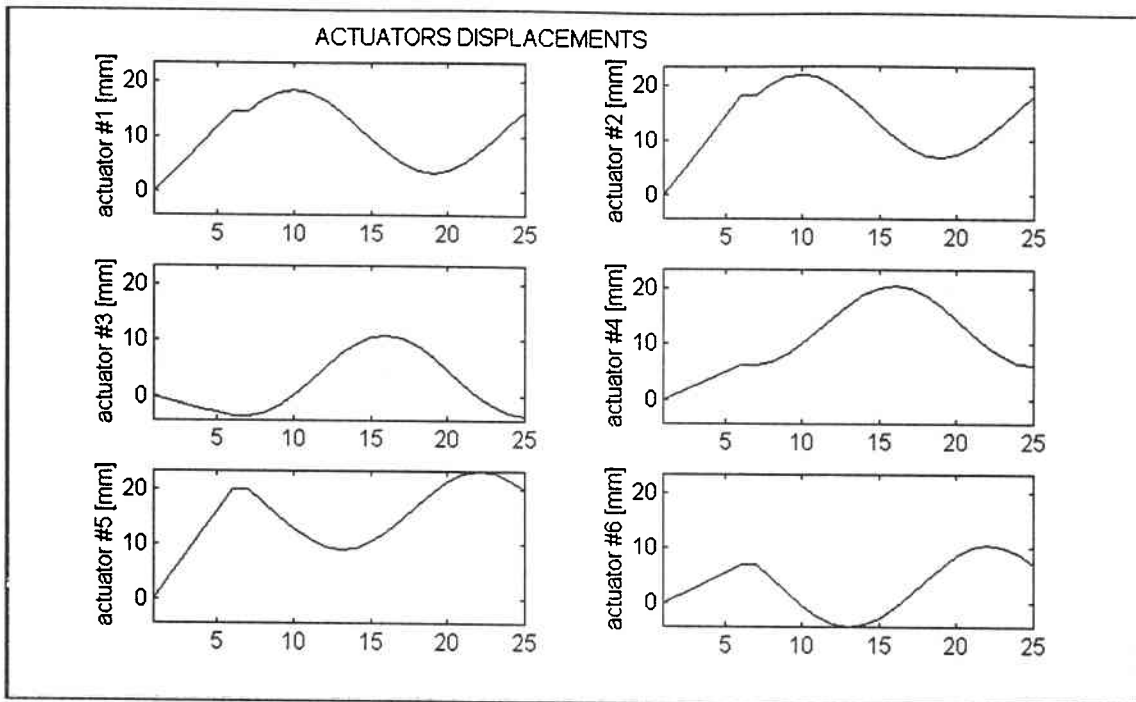
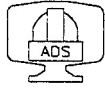


Figure 3. Actuators length variation for 12 mm focus, 9 mm X,Y offset and 1.2 deg cone nutation.

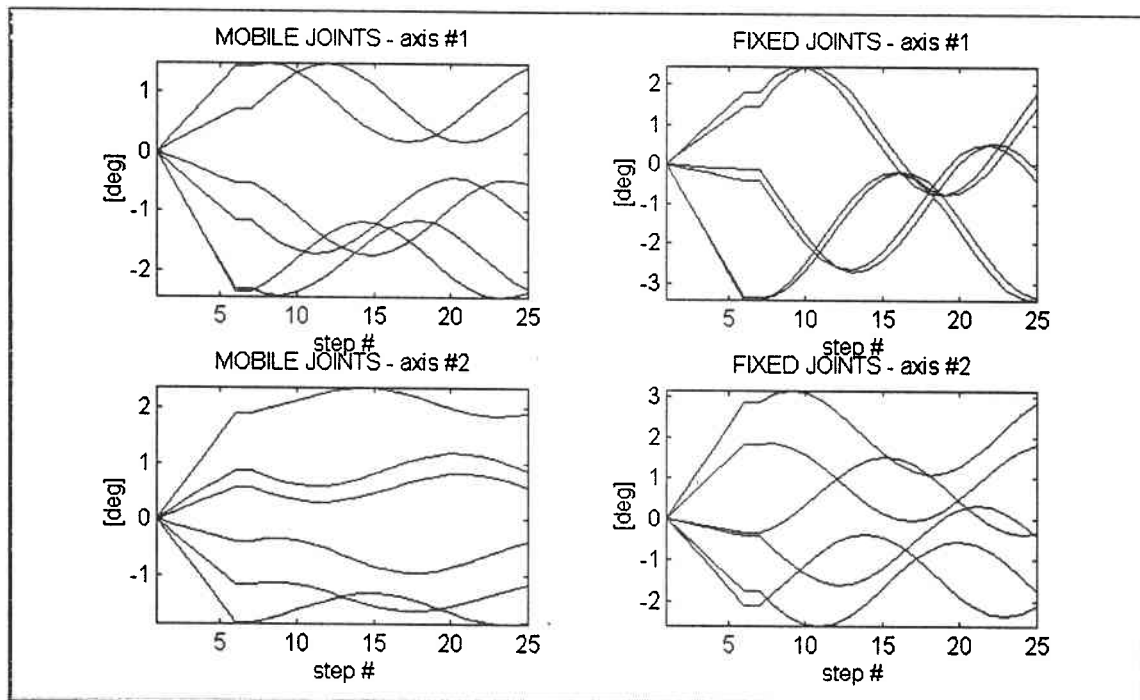
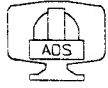


Figure 4. Joints angles variation for 12 mm focus, 9 mm X,Y offset and 1.2 deg cone nutation.



4. JOINTS DESIGN

According to ref.1, the weight of the f/5 secondary mirror system is 6000 N.

The estimated mass of the hexapod, included the fixed and mobile plates, is about 170 Kg.

Actuators axial loads when zenith pointing:

$$1 = 2 = 3 = 4 = 5 = 6 = + 1300 \text{ N}$$

Actuators axial loads when horizon pointing:

$$1 = 2 = + 4121 \text{ N}$$

$$3 = 4 = - 4028 \text{ N}$$

$$5 = 6 = - 93 \text{ N}$$

Figure 5 reports the actuator axial loads as function of telescope elevation.

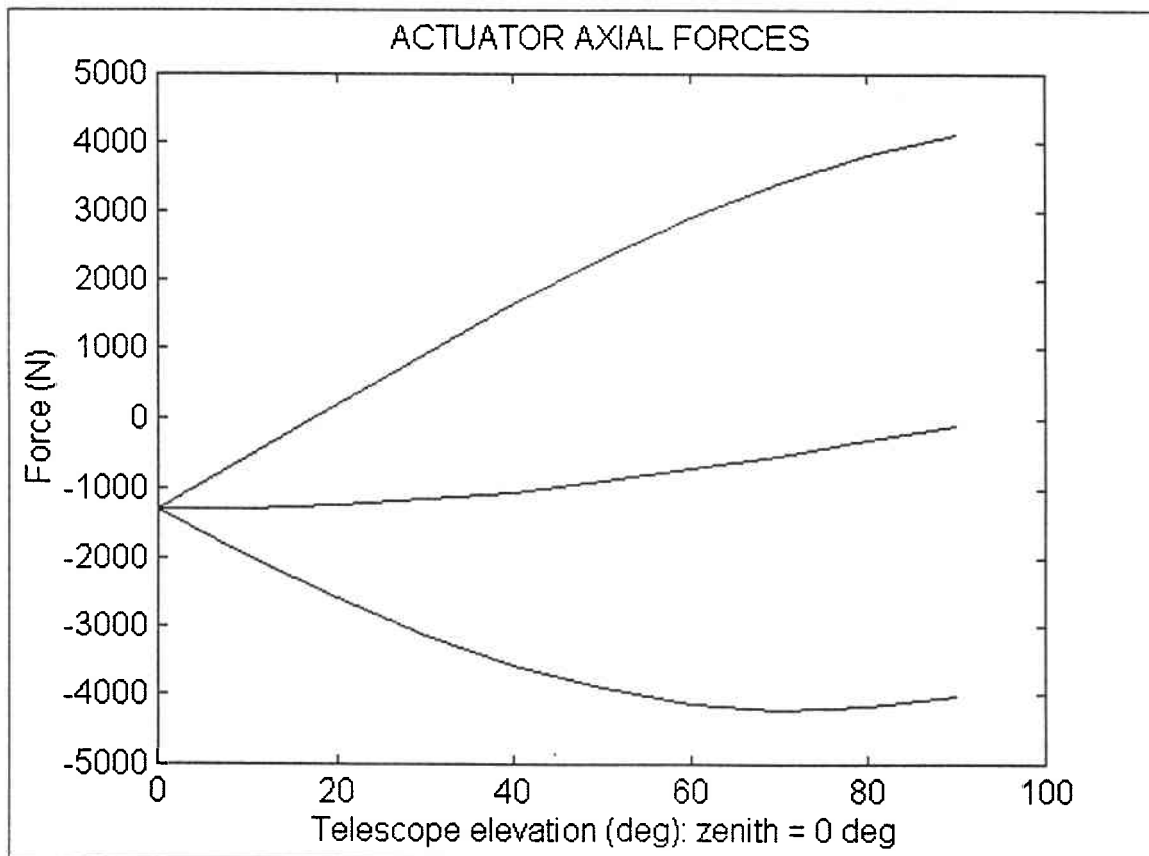
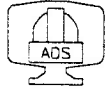


Figure 5. Actuators loading.



Each joint is made by three components: the central cross pinion and two U-shaped flanges carrying the two bearings pairs.

The design axial load is 4500 N.

The bearings are FAG B7000E.T.P4S.UH with a max static loading of 2400 N. Each bracket carries two bearings, thus loaded by 2250 N (static load).

The pin diameter is 10 mm and the bearing height is 8 mm; the minimal flange section at the bearing interface is $2 \times (9 \times 4.5) = 81 \text{ mm}^2$.

Thus, assuming an actuator max axial load of 4500 N, the max structural stress into the joint flange is $\frac{2250}{81} = 28 \text{ N/mm}^2$. The bearing pressure is $\frac{2250}{10 \times 8} = 28 \text{ N/mm}^2$.

The bearings come already preloaded to assure that the universal joint does not introduce play into the hexapod structure. Moreover, further preload is introduced by a flange fixed on the bracket by four screws in order to increase bearing's stiffness with respect to its nominal value.

Figure 6 reports the stress pattern into the universal joint when the 4500 N is applied in the rotated configuration (6 deg on both axes).

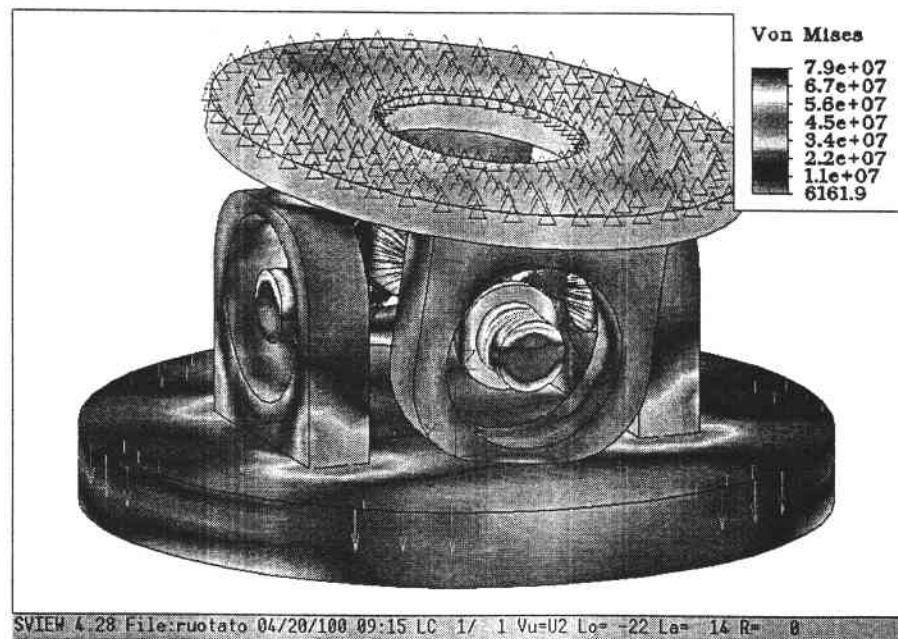


Figure 6. Universal joint stress pattern under 4500 N load.



5. MECHANICAL DESIGN

This paragraph reports the selection of the most relevant actuator mechanical components.

Screw: ROLLVIS Satellite Roller Screw RVR 25 x 1

Nominal diameter $d_0 = 25$ mm

Lead = 1 mm

Dynamic load rating = 12.2 KN - Static load rating = 18.9 KN

Nut stiffness = 605 N/ μ m

Screw stiffness (length 20 mm) = $\frac{21000 \times 10^7 \times \pi (0.025/2)^2}{0.020} = 5152$ N/ μ m

Lead angle = $\varphi = \arctan\left(\frac{P}{d_0 \pi}\right) = \arctan\left(\frac{1}{25 \pi}\right) = 0.73$ deg

Efficiency (%) results smaller than min values, min val. used:

$\eta_1 = (0.68) \rightarrow 0.71$ - force direction opposite to movement

$\eta_2 = (0.58) \rightarrow 0.61$ - force direction toward movement

Preload design:

Max Axial loads on the screw nut = 4500 N

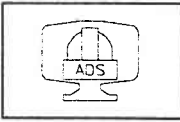
Minimum preload to be applied to the nut = $F_{pr} = 4500 / 2.83 = 1590$ N

Selected preload value = 2000 N

Torque due to preload = $\frac{2000 \times 0.001 \times \left(\frac{1}{0.9 \times 0.71} - 0.61\right)}{2 \pi} = 0.30$ Nm

Max torque for braking: $C_{BRK} = \frac{F_{MAX} \times P}{2 \pi} \times \eta_2 - C_{PRE} =$

$= 4500 * 0.001 / 6.28 * 0.61 - 0.30 = 0.14$ Nm



WARNING: for brake verification it is assumed a null preload torque:

$$\text{Max torque for braking} = 4500 * 0.001 / 6.28 * 0.61 = 0.44 \text{ Nm}$$

Backdriving force:

$$C_{BCK} = \frac{F_{BCK} \times P}{2\pi} \times \eta_2 = C_{PRE} \rightarrow F_{BCK} = 0.30 \times 6.28 / 0.001 = 1884 \text{ N}$$

Demanded torque for lifting:

$$T_{lif \max} = \frac{4500 \times 0.001}{2\pi \times 0.71} = 1.01 \text{ Nm}$$

Demanded torque for lowering:

$$T_{low \max} = \frac{4500 \times 0.001 \times 0.61}{2\pi} = 0.44 \text{ Nm}$$

Demanded torque for accelerating the rotating masses:

considering the extremely small value of the specified axial speed 0,5 mm / sec = 30 rpm of the motor, the angular acceleration is very small and the accelerating torque can be neglected in the balance of the max. torque demanded to the motor.

Total demanded torque: C = 1.01 + 0.3 = 1.31 Nm

Motor: Inland Brush servomotor QT Series, type 2603

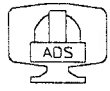
Motor Constant	= 0.28 lb ft / sqrt(W)	= 0.38 Nm/sqrt(W)
Peak Torque	= 5 lb ft	= 6.78 Nm
Inertia	= 4x10 ⁻⁴ lb ft s ²	= 1.09x10 ⁻⁴ Kg m ²
Weight	= 3.5 lb	= 15.6 N

Brake: Electroid Failsafe brake EFSB Series, type EFSB35

Rated static torque	= 35 lb in	= 3.95 Nm
Inertia	= 0.127 lb in ²	= 3.5x10 ⁻⁵ Kg m ²
Weight	= 2.7 lb	= 12 N

Encoder: Heidenhain Incremental Encoder type ERO 1324

angular resolution	= 5000 line counts /rev (x 4)
resolution on 1 mm pitch screw	= 0,05 μm/cts



LVDT SENSOTEC BY132HQ

DC-DC long stroke LVDT

Captive guided spring return

Stroke range $\pm 1.0''$

5.1 – Actuator stiffness

According to the dwg 301005 the most relevant contribution to the actuator axial stiffness is given by the Aluminum frame components and by the mechanical items.

The Al frame components are:

- encoder housing: AL cylinder diam=86mm h=40mm t=9mm => 4300 N/um
- motor housing: AL cylinder diam=86mm h=70mm t=6mm => 1650 N/um
- nut housing: AL cylinder diam=67mm h=85mm t=10mm => 1750 N/um

For the commercial items as nut screw and bearings the stiffness rates come from the Catalogue's Supplier.

Joints = 100 N/ μ m (this is an indicative value and depends on the bearings preload that could be further increased)

Nut = 605 N/ μ m

Bearings = 158 N/ μ m (axial stiffness catalogue value for one pair of B7205E.T.P4S with high preload)

The series of the above mentioned items is:

$$K = 1/(1/4300+1/1650+1/1750+2/100+1/605+1/158) = 34 \text{ N/um}$$

The overall stiffness of the actuator is $K_{ax} = 34 \text{ N/um}$.

6. FINITE ELEMENTS ANALYSIS

This analysis is devoted to identify hexapod contribution to the M2 f/5 unit static and dynamic responses.

The actuators are modelled as rod elements.

The joints are modelled as spherical hinges between the actuators end and the interface blocks on the flanges.

The actuator properties are derived from the actuator mechanical values.

$$A = K_{ax} \times L / E = 50 \times 10^6 \times 0.383 / 21000 \times 10^7 = 91.2 \times 10^{-6} \text{ m}^2 \approx 91 \text{ mm}^2$$

$$\text{The mass density is: } \gamma = M / (A \times L) = 14 / (91.2 \times 10^{-6} \times 0.383) = 4.44 \times 10^5 \text{ Kg/m}^3$$

The actuators torsion and bending moments of inertia are not accounted for.

The F.E. model consists of:

<u>item</u>	<u>mass [Kg]</u>
- actuator	= 15.5 (including cardan joints)
- interface wedge	= 8 (on fixed plate) , 11 (on mobile plate)
- hexapod flange	= 13.1 (fixed plate) , 14.3 (mobile plate)
- mirror	= 600

Two different models are analysed: the *hub unit* and the hub attached to the spiders, named *top-ring unit*.

The *hub unit* consisting of optical subsystem plus the hub weighs 11156 N. This model is restrained at the hub interfaces with the spiders.

The *top-ring unit* includes the spiders effect as well. The overall weight is 14069 N. The spiders are described by adopting beam elements with the geometrical and cross-sectional features as seen from "S-2" and "S-3" MMT dwgs.

The ends of the spiders connecting to the telescope top ring are fixed to ground.

All the spiders beams are modelled by one single element between each crossing, in order to hide their local modes from the structural modes of the *top ring unit*.

This trick allows obtaining only the global structural modes, thus skipping the local ones of the spiders. Of course, even if not listed, the local modes do occur.

The four hub support straps are preloaded to achieve an overall tensile load of 9748 N and 11600 N for the top and bottom ones respectively, when zenith pointing.

Such internal stress pattern is then the sum of the actual preloading and the effect of the hub own weight.

The additional removable hub support struts are not preloaded.

6.1 – Static Analysis

The displacements of the mirror CG are computed as function of the telescope elevation.

Table 2 reports the *hub unit* results and table 3 reports the *top ring* model ones.

Elev. (deg)	X CG disp. (mm)	Y CG disp. (mm)	Z CG disp. (mm)
90	0	-	-0.077
60	0.191	-	-0.067
30	0.331	-	-0.039
0	0.382	-	0

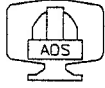
Table 2 – *hub unit* static analysis. Mirror CG displacements.

Elev. (deg)	X CG disp. (mm)	Y CG disp. (mm)	Z CG disp. (mm)
90	0	-	-19.42
60	0.657	-	-19.19
30	1.141	-	-18.56
0	1.318	-	-17.70
spider preload	-	-	-17.70

Table 3 – *top ring unit* static analysis. Mirror CG displacements.

The largest contribution to the mirror displacement is given by the spider preloading.

In fact, the “z” displacement due to the spider preload case matches the one of the telescope horizon pointing case.



6.2 – Modal Analysis

Table 4 reports the most significant natural frequencies of the *hub unit* alone and table 5 shows the *top-ring* model results.

Mode	Freq. (Hz)
1 – h5 lateral	24.8
2 – h5 lateral	24.9
3 – h5 torsional	40.9
4 – h5 piston	63.9

Table 4 – *hub unit* modal analysis.

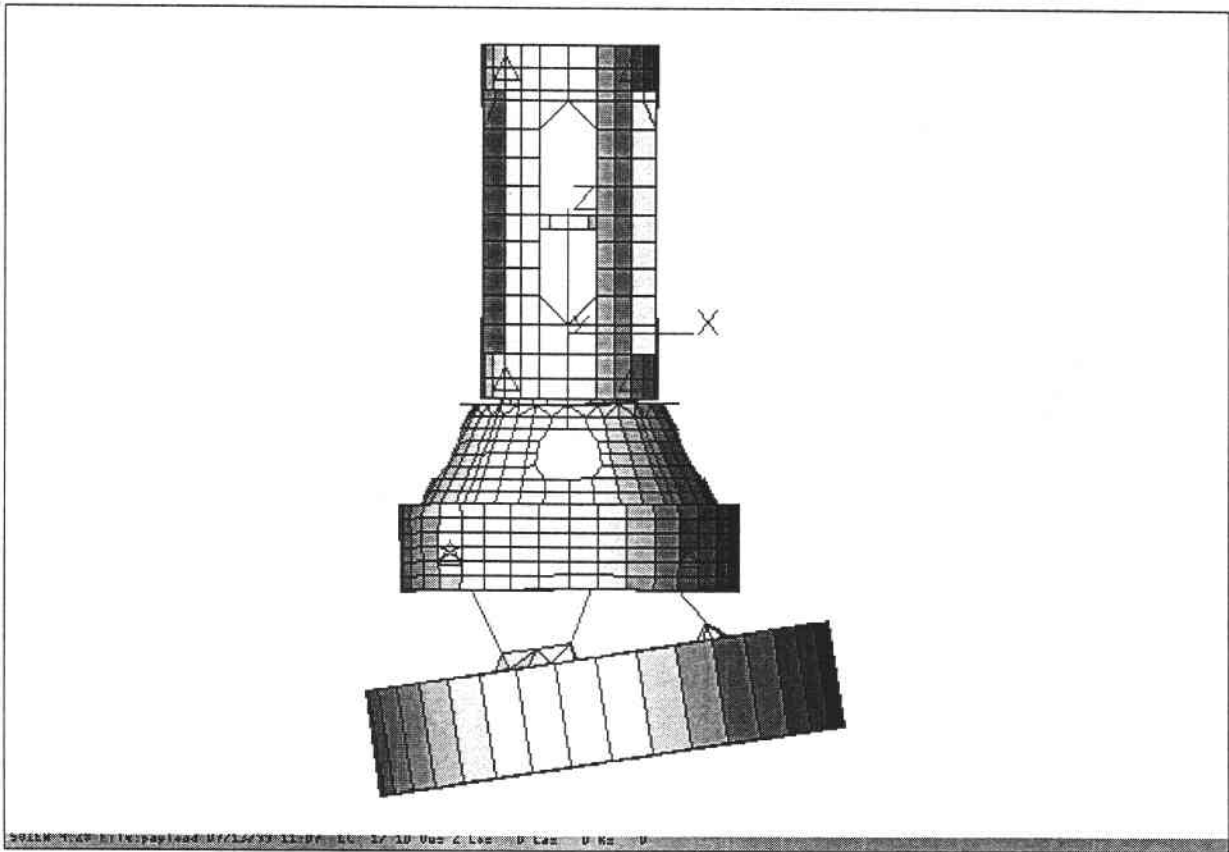
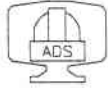


Figure 7. *hub unit* 1st mode (24.8 Hz).



Mode	Freq. (Hz)
Torsion	6.31
Piston	12.8
1 st bend	14.5
1 st bend	14.5
Spider bend.	40.5
Spider bend.	40.6

Table 5 – top ring unit modal analysis.

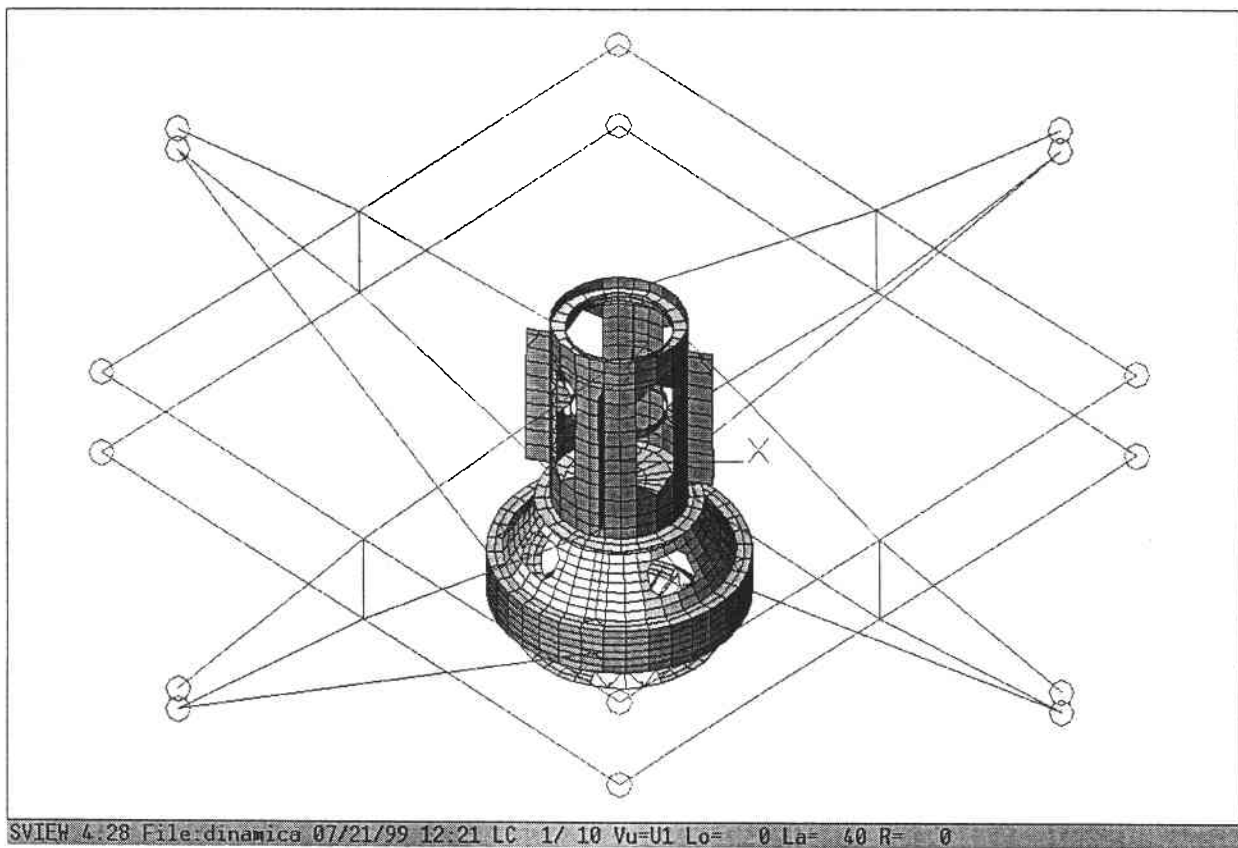


Figure 8. top ring unit 1st mode (6.31 Hz).

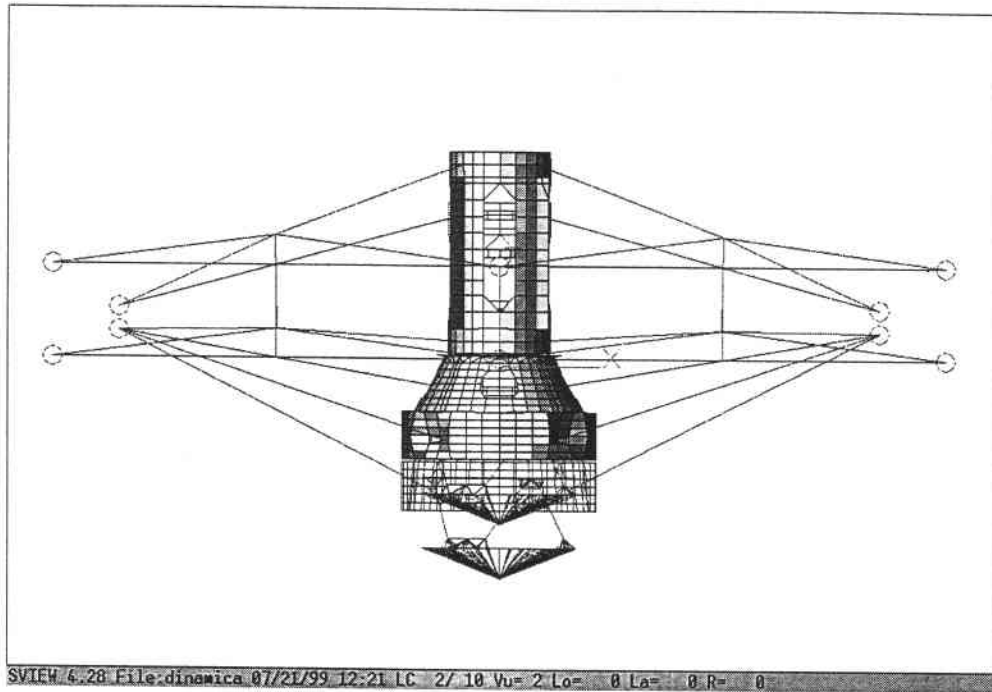
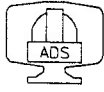


Figure 9. *top ring unit* piston mode (12.8 Hz).

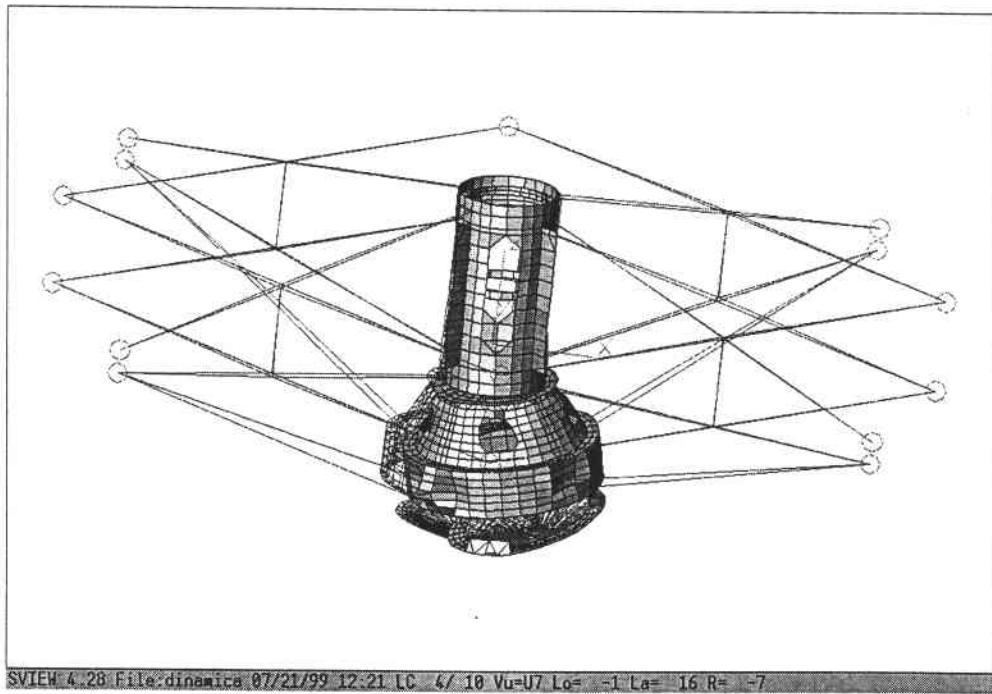




Figure 10. *top ring unit* mode @ 14.5 Hz.

	MMT CONVERSION	Doc.No: H5-RP-AD-99001 Issue : E Date : 17 May 2000	
---	-----------------------	---	---



7. FINAL REMARKS

The f/5 hexapod design has been carried out based on the f/15-f/9 unit one.

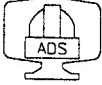
Flexure joints have been replaced by universal ones (cardans with ball bearings) to deal with increased load and larger rotations.

The mechanical figures of the hexapod have been analysed in the frame of the MMT top ring system.

The SOW stroke specifications result fulfilled individually, while the simultaneous combination of the three different shifts is restricted by the actuator and LVDT maximum stroke.

	MMT CONVERSION	Doc.No: H5-RP-AD-99001 Issue : E Date : 17 May 2000	
--	-----------------------	---	--

ANNEX 1

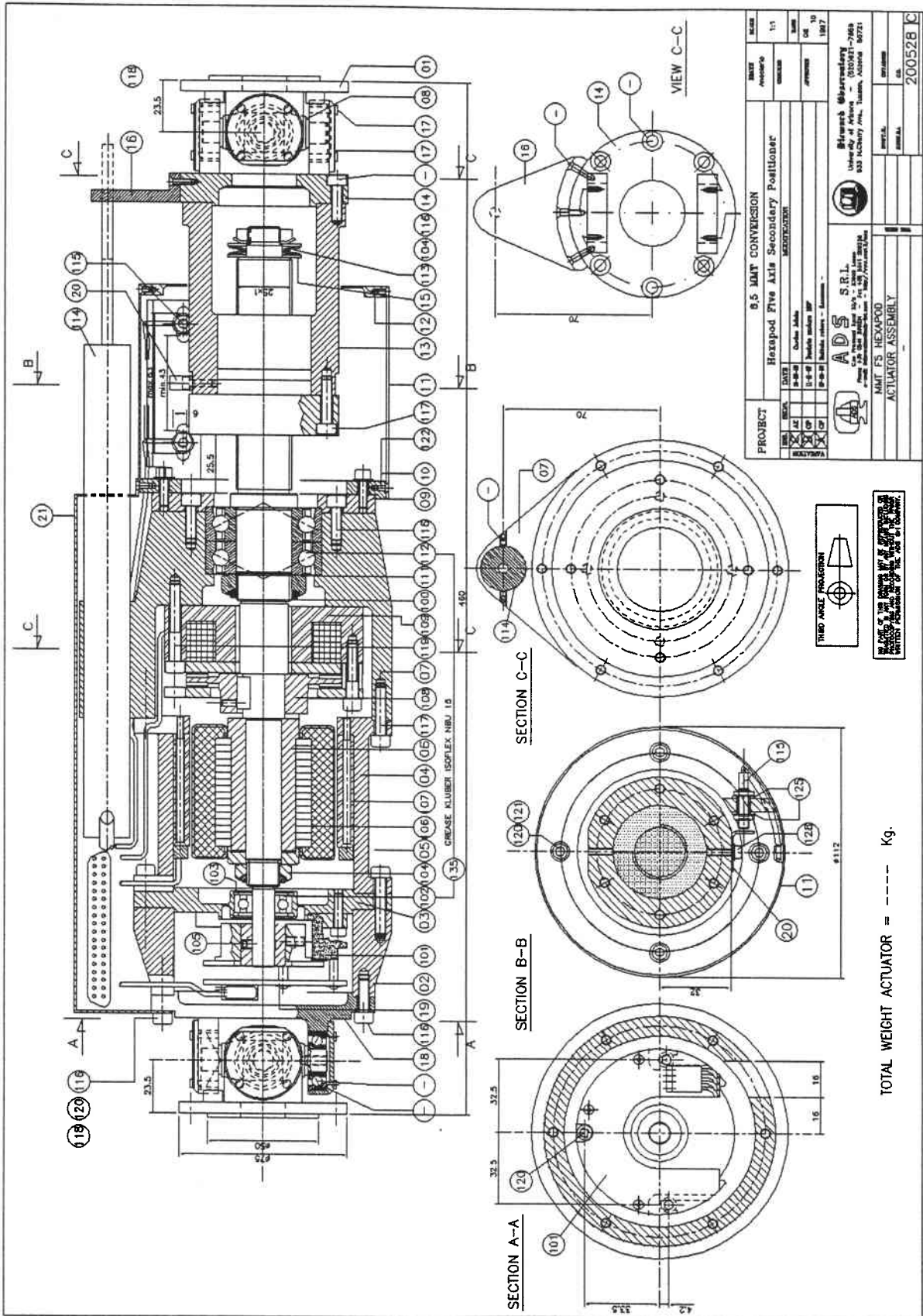


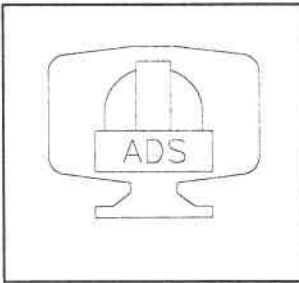
MMT CONVERSION

Doc.No: H5-RP-AD-99001

Issue : E

Date : 17 May 2000





MMT CONVERSION

Doc.No. : H5-TR-AD-01001
Issue : A
Date : 21 April 2001



Steward Observatory

MMT CONVERSION

SECONDARY MIRRORS SUPPORT

M2/F5 HEXAPOD TEST REPORT

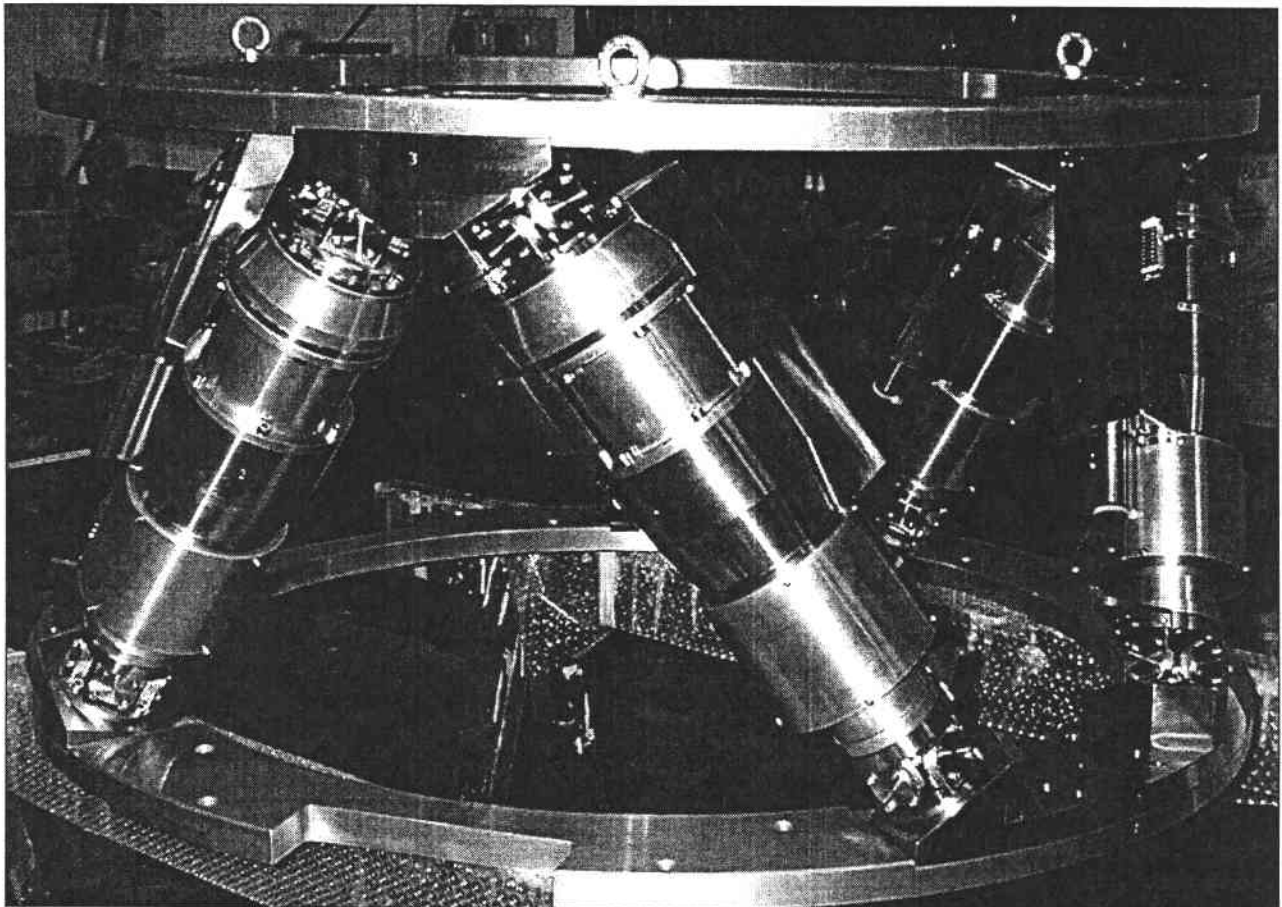








TABLE OF CONTENTS

1. INTRODUCTION	4
2. TEST SETUP	5
2.1 Bench stiffness	6
3. TEST PROCEDURE	7
3.0 Installation and calibration	7
3.1 Stiffness	7
3.2 LVDT linearization	8
3.3 Screw lead error	8
3.4 Repeatability	8
3.5 Resolution	9
3.6 Backlash	9
3.7 Step response	10
3.8 Power consumption	10
4. TEST RESULTS	11
4.1 Stiffness	11
4.2 LVDT calibration	14
4.3 Screw lead error	19
4.4 Repeatability	23
4.5 Resolution	24
4.6 Backlash	25
4.7 Step response	29
4.8 Power consumption	32
5. HP TESTS	34
5.1 Weight	34
5.2 Distance between the plates	34
5.3 Axial stiffness	35
6. FINAL REMARKS	37

	<p>MMT CONVERSION M2 f/5 HEXAPOD</p>	<p>Doc.No: H5-TR-AD-01001 Issue : A Date : 21 April 2001</p>	
---	--	--	---

APPLICABLE DOCUMENTS AND REFERENCES

1. Statement of Work (SOW), "The f/5 hexapod positioning system for the MMT Conversion Project", March 2nd 1999;
2. H5-RP-AD-99001, "M2/F5 Hexapod design report", Issue E dated 17 May 2000.

	MMT CONVERSION M2 f/5 HEXAPOD	Doc.No: H5-TR-AD-01001 Issue : A Date : 21 April 2001	
---	--	---	---

1. INTRODUCTION

This document reports on the test and calibration of the linear actuators of the hexapod supporting the f/5 secondary mirror.

The tests have been performed at ADS premises during the period Jan.–April 2001.

Section 2 describes the test procedure and section 3 reports the results for the seven actuators.

The following tests have been performed on each actuator:

1. stiffness;
2. LVDT calibration;
3. screw lead error;
4. repeatability;
5. resolution;
6. backlash;
7. step response;
8. power consumption.

Finally, some measurements made on the integrated Hexapod are reported as well.



2. TEST SETUP

The test setup consists of a test bench that holds one actuator at a time and allows to measure its response under different loading conditions.

The test bench embeds a linear encoder Heidenhain model MT101M with a stroke of 100mm and an interpolated resolution of 0.1 μm .

The actuator is controlled by a PMAC industrial controller and it is powered by a Trust Automation TA115 driver.

All the tests are executed by a command program running in Visual Basic environment which is linked to the PMAC controller through a serial line.

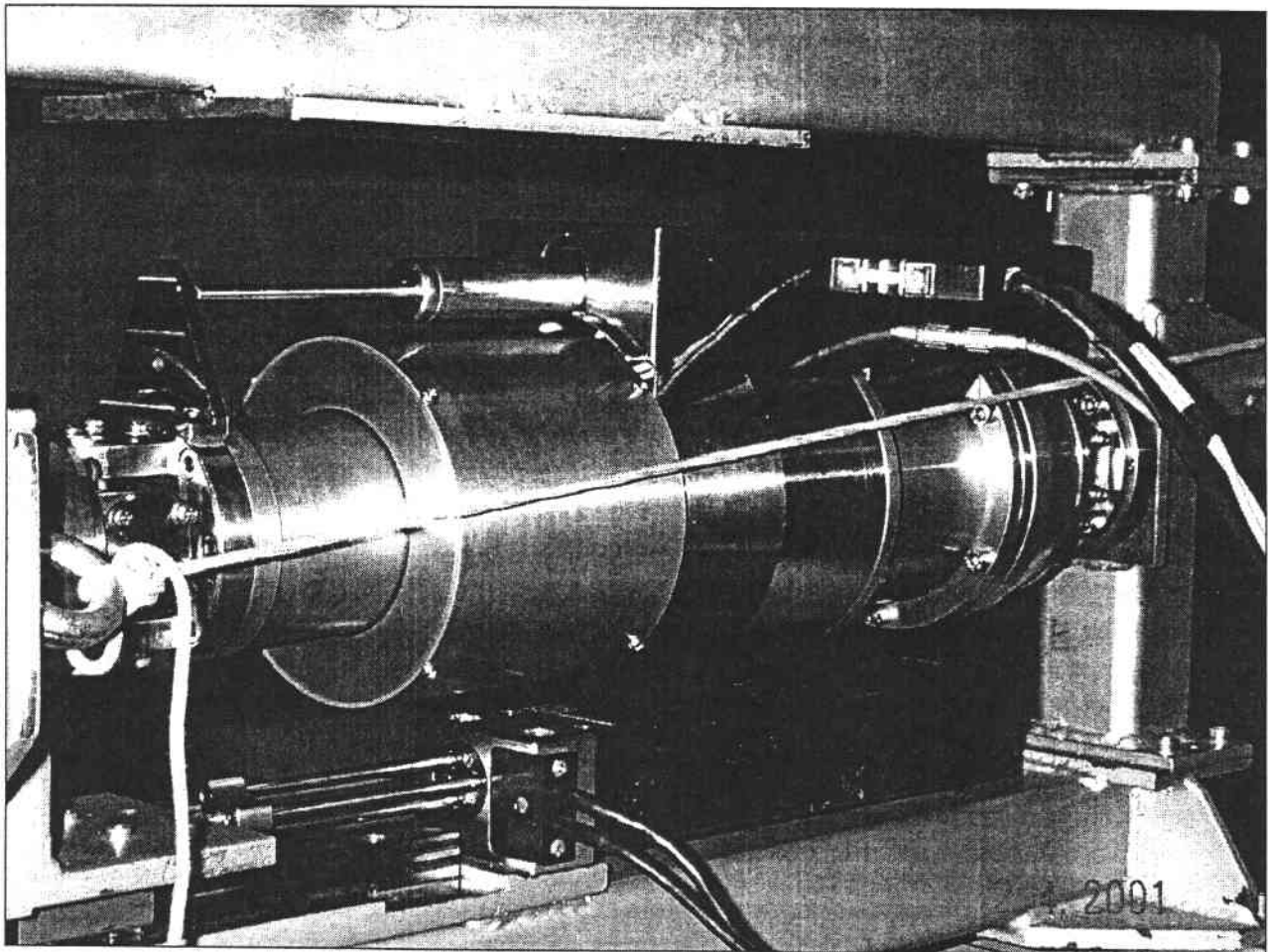


Figure 1 – Test setup.

2.1 Bench stiffness

The measurements of the actuator stiffness need to be reduced by accounting for the test bench own stiffness.

To derive the stiffness of the of the test bench a dummy beam of known stiffness is installed in place of the actuator and the global stiffness is measured.

The stiffness of the dummy that can be computed from the beam's theory is

$$K_{\text{dummy-th}} = E A / L = 21 \times 10^{10} \pi 0.015^2 / 0.5 = 297 \text{ N} / \mu\text{m}$$

while the stiffness derived from the FE method, clamping the beam's ends as it happens in the actual conditions,

$$K_{\text{dummy-FEA}} = 246 \text{ N} / \mu\text{m}.$$

that will be used for the further calculations.

The bench stiffness can be computed by supposing that the measured K_{TOT} value is due to the series of two different elastic elements: the bench and the dummy.

The measured value is $K_{\text{TOT}} = 39.8 \text{ N}/\mu\text{m}$.

Thus,

$$K_{\text{bench}} = K_{\text{dummy}} \times K_{\text{TOT}} / (K_{\text{dummy}} - K_{\text{TOT}}) = 246 \times 39.8 / (246 - 39.8) = 47.4 \text{ N}/\mu\text{m}$$

This value will be used to subtract the bench contribution to the overall stiffness measured for the bench plus the actual actuator.

3. TEST PROCEDURE

This section reports the procedure that has been followed to calibrate and test all the seven linear actuators.

All these tests are run at ambient conditions, that is 20..22°C and 35..45% humidity.

3.0 Installation and calibration

The two end joints interface flange must be bolted on the bench frame by properly recovering the rotation play that is produced by the gap between the four screws and the pass holes of the flanges.

WARNING: when tightening the four screws, each joint must be turned clockwise looking at it from the actuator side.

This is required to keep the correct gap between the limit switches sensing head and the reference frame.

Such procedure must be followed when installing each actuator into the Hexapod as well.

3.1 Stiffness

The stiffness test is performed at two different position of the actuator:

1. actuator extended = 22 mm from mid stroke;
2. actuator closed = -22 mm from mid stroke.

For each one of these conditions, the loading-unloading procedure is repeated three times:

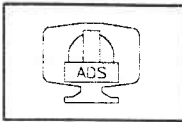
Step #	1	2	3	4	5	6	7
Load [N]	-79	-29	20	69	88	108	128

Table 1 – Stiffness test load sequence.

The average slope (in the least square sense) of the collected data are then reduced by using the stiffness value obtained for the bench, that is K_{bench} (47.4 N/μm).

The actual stiffness of the actuator is computed as:

$$K_{\text{act}} = K_{\text{bench}} \times K_{\text{ALL}} / (K_{\text{bench}} - K_{\text{ALL}})$$



3.2 LVDT linearization

This test has been performed in order to investigate the LVDT linearity and find the optimal LVDT linearization factor in ambient condition when the transducer is powered at its nominal voltage (30.00 V).

The aim is also to estimate the absolute error that should occur if using the LVDT as an absolute sensor to close the position control loop.

The test procedure is performed by recording the LVDT readings in the sequence described in 3.3.

3.3 Screw lead error

This test is aimed to measure the screw average lead at ambient temperature.

Starting from -23 mm, a sequence of 1/3 mm pitch is commanded up to +23 mm on the base of rotary encoder commands.

The error that is measured between the given rotary command (read by the rotary encoder itself) and the linear displacement read by the linear optical reference gives the screw lead error.

3.4 Repeatability

In the repeatability test, eight different positioning commands are sent to the actuator in order to cover most of the its stroke: starting from the -20 mm position, the following absolute positions are commanded:

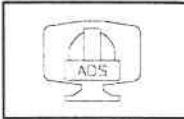
Step #	1	2	3	4	5	6	7	8
Actuator stroke (mm)	5	10	15	20	25	30	35	40

Table 2 – Repeatability test sequence: the stroke is measured from the closed position, that is -20 mm from actuator nominal length.

Each one of the eight positions, hereafter referred as “XX”, is commanded five times following this procedure:

1. go to - 22 mm;
2. go to - 21 mm;
3. go to - 20 mm;
4. reset the linear external reference to zero;
5. go to “XX”;
6. store the linear external reference position;

The approaching steps 1 to 3 are useful to cancel possible plays of the sliding unit due to the inversion of the motion.



The results test are summarised as PTV variation in the reached positions. The constant part of the positioning error is clearly due to the mean lead error and should be properly compensated.

3.5 Resolution

The resolution test is performed in order to measure the capabilities of the system to drive small displacements commands. Five commands are sent to the actuator starting from 5 μm down to 1 μm amplitude. All the commands are provided in terms of encoder counts while the actual displacement is measured by the external linear reference that is reset before each one of the five commands.

3.6 Backlash

The test consists in the following sequence:

1. Store position 1;
2. Forward step (+100 μm);
3. Backward step (-100 μm);
4. Store position 2;
5. Compare positions 1 and 2.

The test is performed twice at three different actuator positions that are, namely:

1. extended, that is 20 mm from the mid stroke;
2. mid stroke;
3. closed, that is -20 mm from the mid stroke.

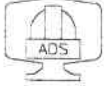

The displacements are taken both in terms of the internal LVDT readings and the external linear encoder readings.

Despite the higher accuracy and resolution of the optical external reference, the backlash will be evaluated by using the internal reading of the LVDT.

In fact, the sliding unit of the test bench (that carries one end of the actuator) seems to be more sensitive to this inversion of the movement than the actuator itself. In this sense, the external reading that is taken at the base of the sliding unit and far from the actuator axis seems to be strongly affected by the sliding unit own elasticity.

In order to decrease the noise that affects the LVDT information (see Sensotec data sheet), the converted output of the sensor has been averaged over a 2000 samples set sampled at 2 kHz.

No load is applied to the actuator during test.

	<p style="text-align: center;">MMT CONVERSION M2 f/5 HEXAPOD</p>	<p>Doc.No: H5-TR-AD-01001 Issue : A Date : 21 April 2001</p>	
---	--	--	---

3.7 Step response

The speed performances of the actuator are evaluated by commanding a + 0.1 mm step (1440 cts) while a 250 N tension load is applied. Position and velocity are recorded as function of the time.

3.8 Power consumption

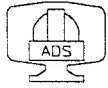
The power consumption of the system is measured by reading the DC current absorbed from the electrical power supply (17 V) during the cruise motion at nominal speed (2 mm/s).

It is important to remember that the absorbed current includes 0.2 A for the braking system plus 0.45 A for the driver in "enable" condition.

Two conditions are studied:

1. actuator travelling at nominal speed with no load applied;
2. actuator travelling at nominal speed lifting 700 N load.

In this way it is possible to separate the power requirements of the pre-loaded system only from the ones of the actual payload.



4. TEST RESULTS

This section reports the results of the measures carried out on the seven linear actuators. Actuator # 7 is left as the spare one.

4.1 Stiffness

For each actuator the results of the stiffness test are presented both for the extended and closed position.

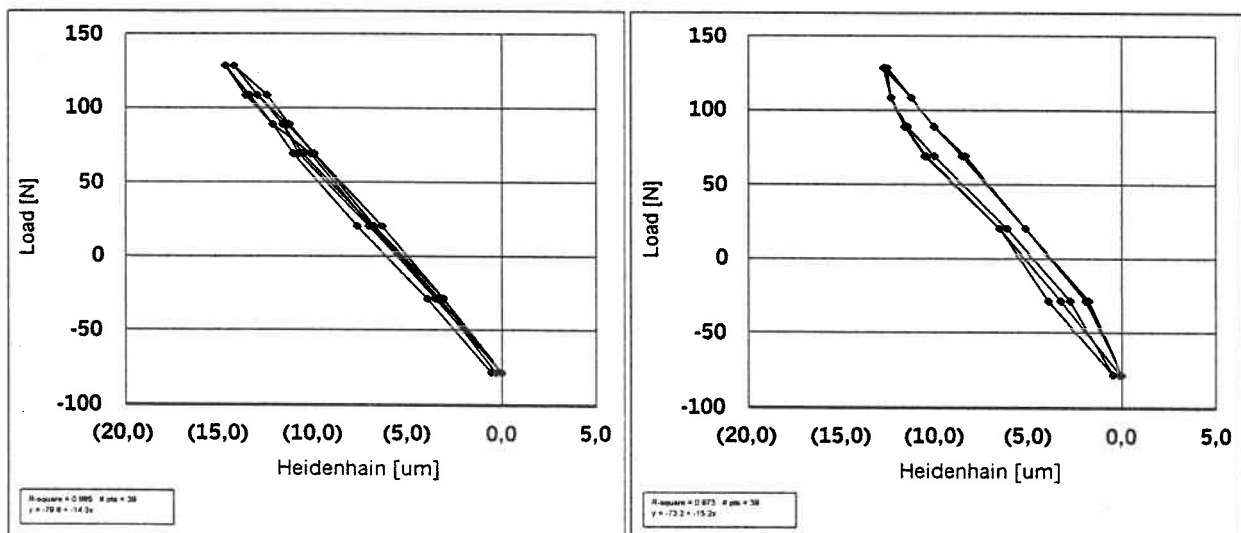


Figure 2 – Actuator #1 stiffness measurements: closed and extended positions.

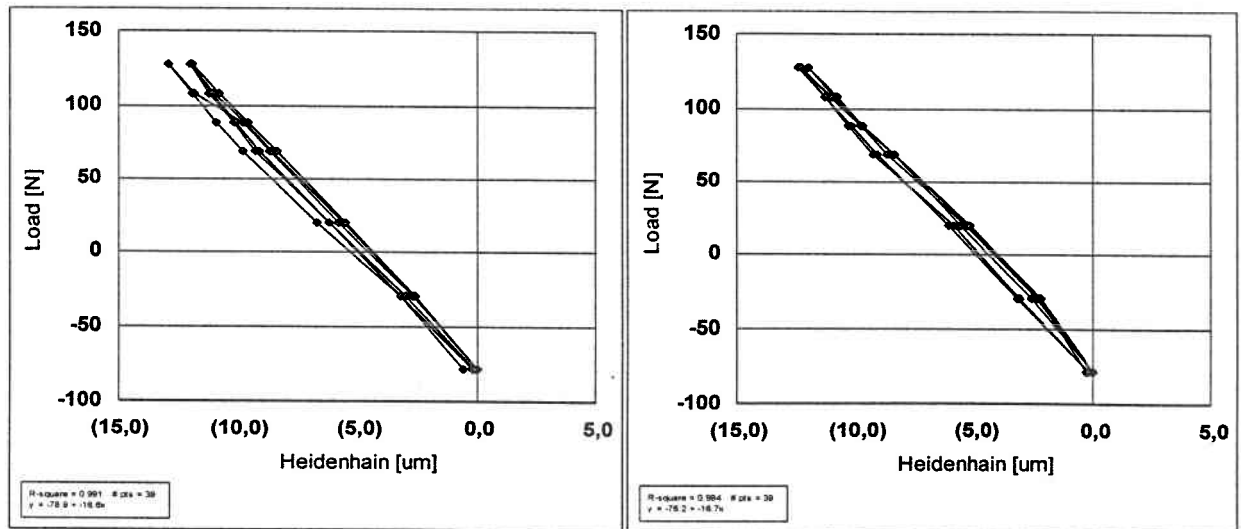


Figure 3 – Actuator #2 stiffness measurements: closed and extended positions.

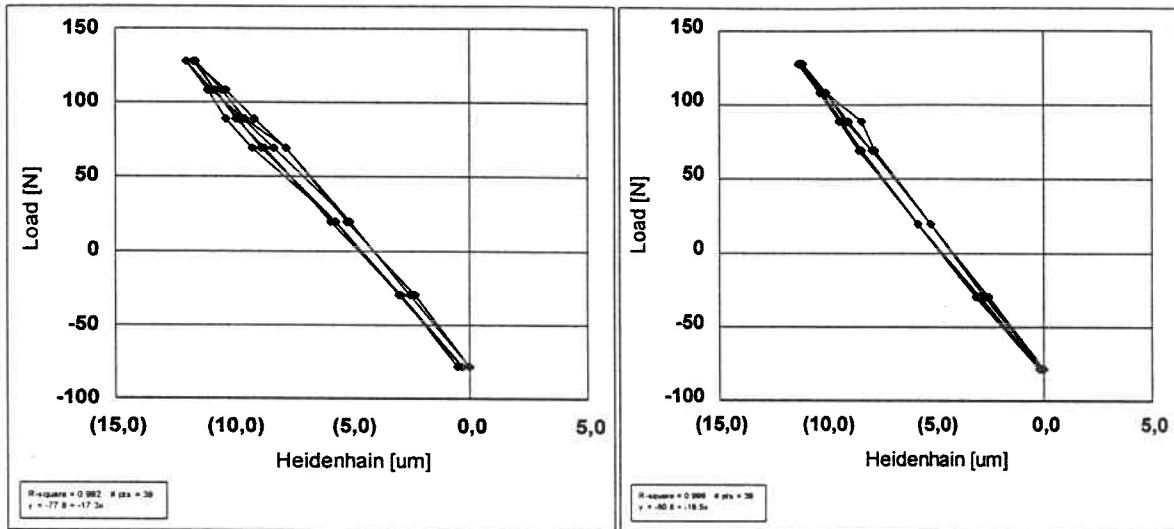
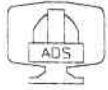


Figure 4 – Actuator #3 stiffness measurements: closed and extended positions.

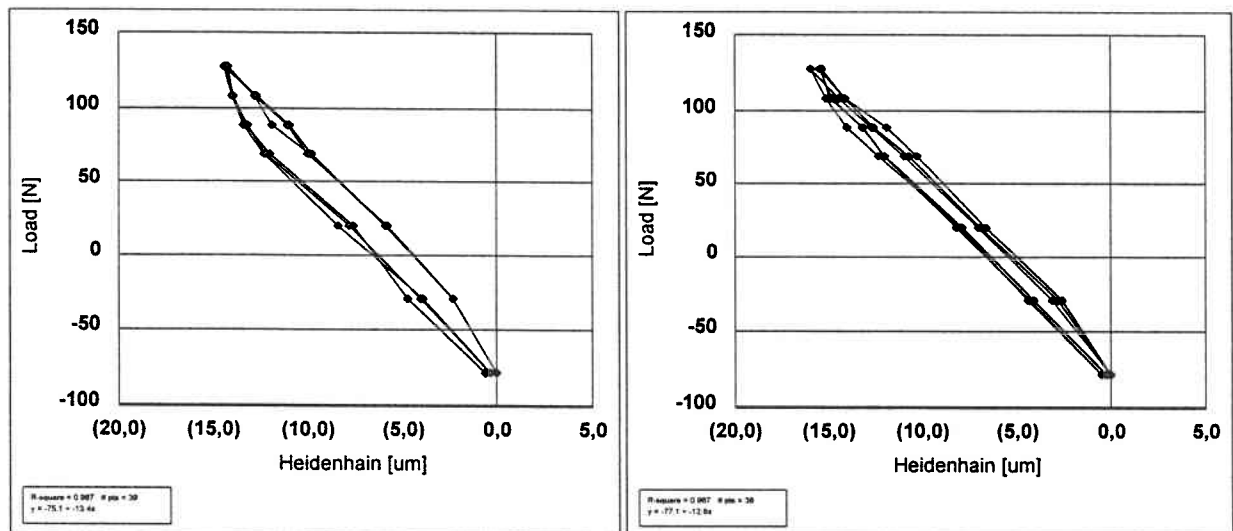


Figure 5 – Actuator #4 stiffness measurements: closed and extended positions.

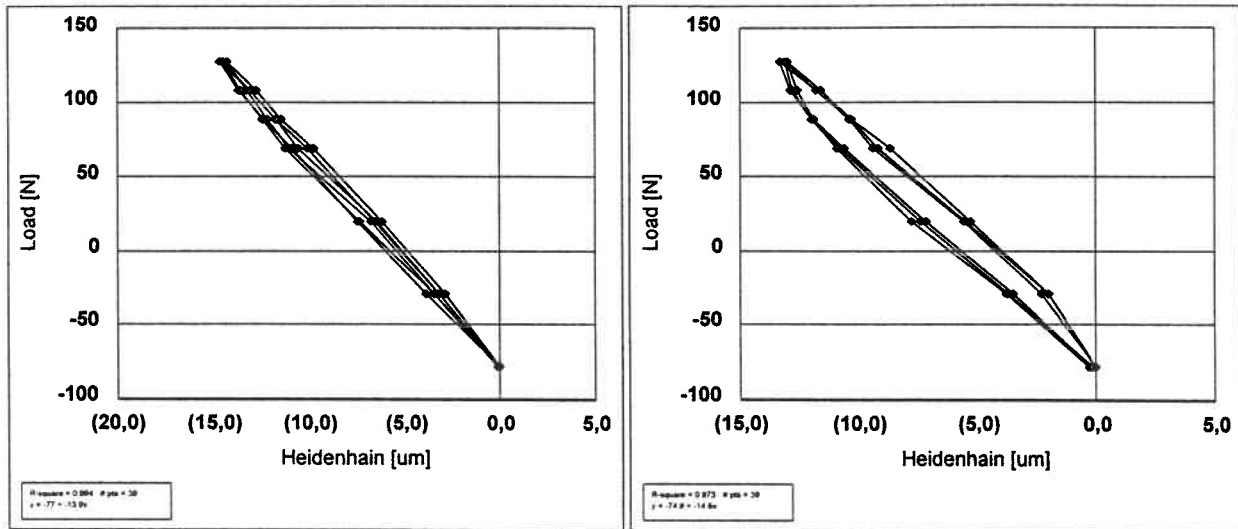


Figure 6 – Actuator #5 stiffness measurements: closed and extended positions.

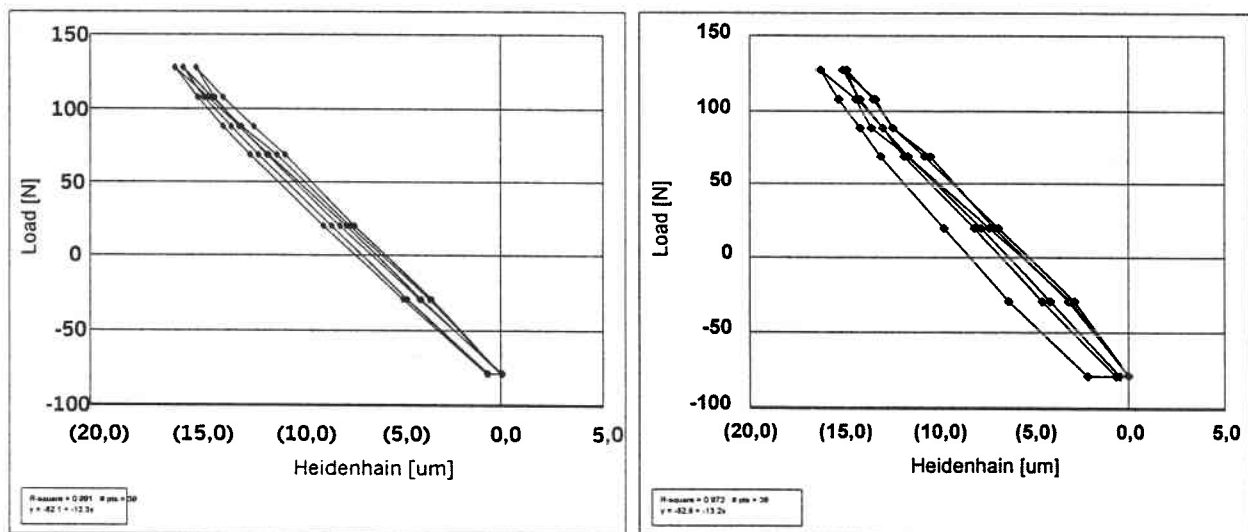


Figure 7 – Actuator #6 stiffness measurements: closed and extended positions.

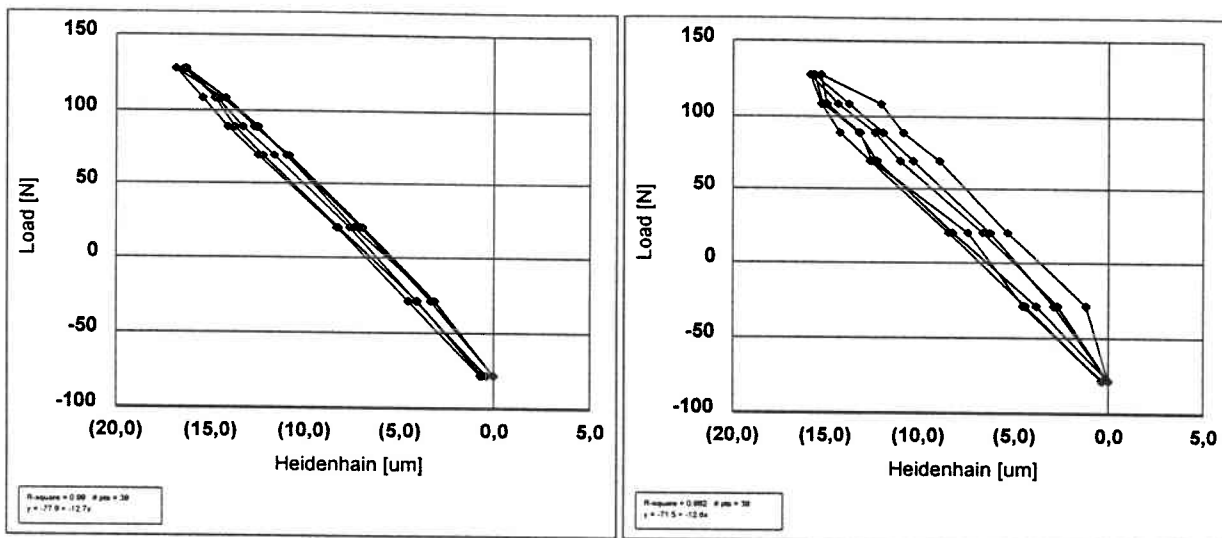


Figure 8 – Actuator #7 stiffness measurements: closed and extended positions.

Table 3 summarises the stiffness values (least square fitting) of all the actuators where the bench own stiffness has already been removed.

Act. #	1	2	3	4	5	6	7
N/ μ m	21.4(*)	25.8	28.8	18.1(*)	20.6(*)	18.4(*)	17.3(*)

Table 3 – Actuators axial stiffness. These values are obtained from the measured slopes by subtracting the bench own stiffness.

(*) The stiffness of this actuator has been measured before augmenting the universal joints bearings preload.

4.2 LVDT calibration

Apart from the thermal stability of the zero and of the slope of the linearization curve, for which a real time compensation should be implemented when using the hexapod in operating conditions, particular attention must be spent on the deviation from the linearity.

The LVDT sensors that have been embedded into the actuators have a good linearity level, but the performances are not good enough for the demanded accuracy.

In the following plots the LVDT output voltage of the sensors is reported as a function of the actuator position measured by the external linear reference.

The standard deviation from the linearity is summarised in the legend of each plot.

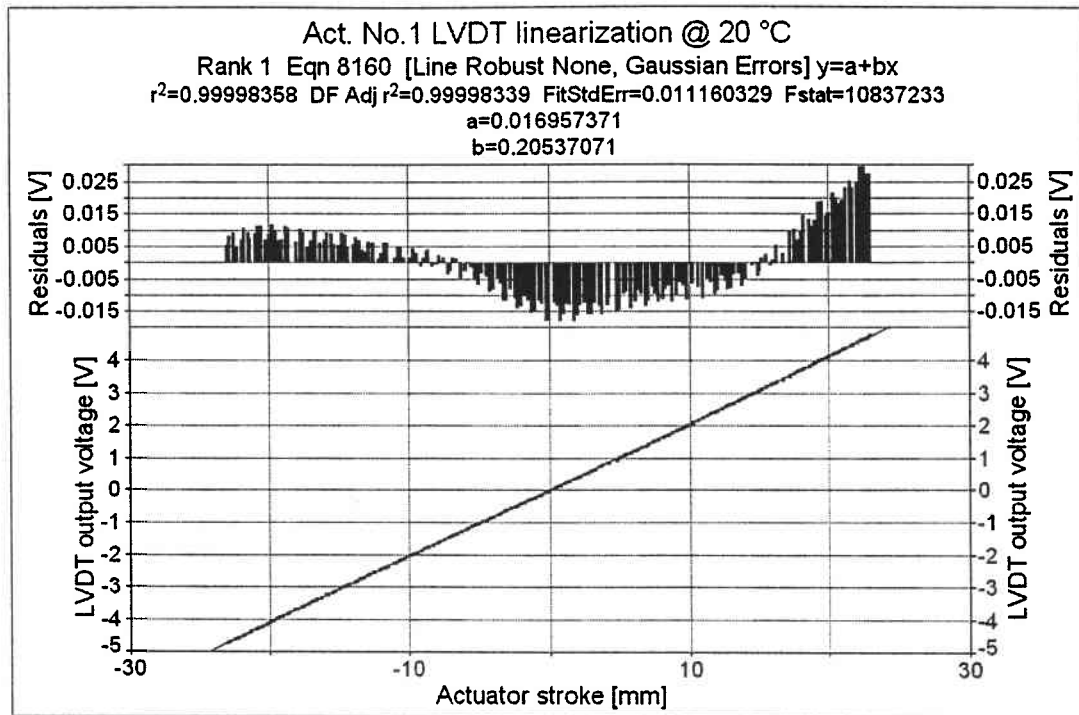
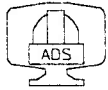


Figure 9 – Actuator #1 LVDT calibration curve.

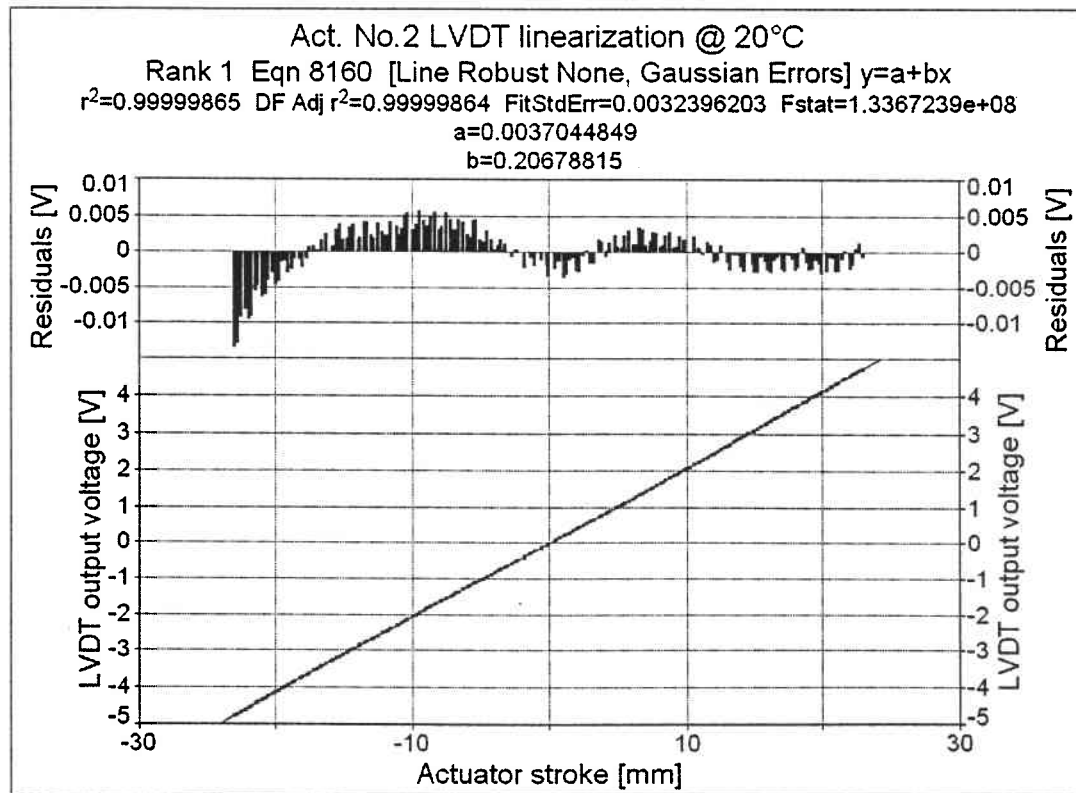


Figure 10 – Actuator #2 LVDT calibration curve.

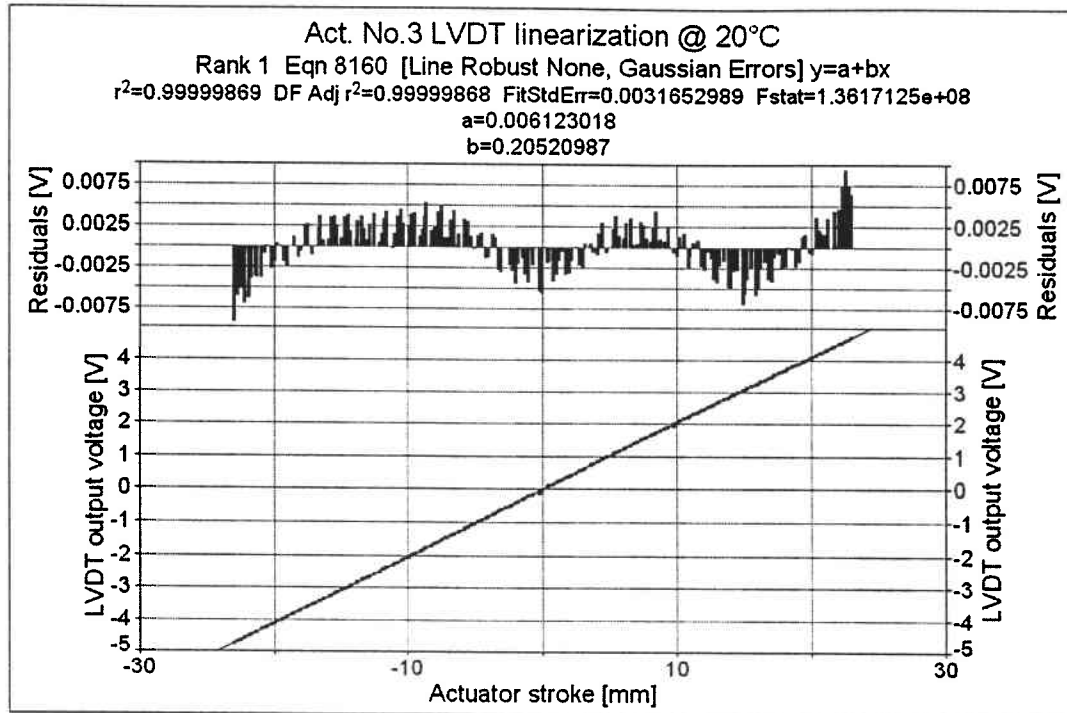


Figure 11 – Actuator #3 LVDT calibration curve.

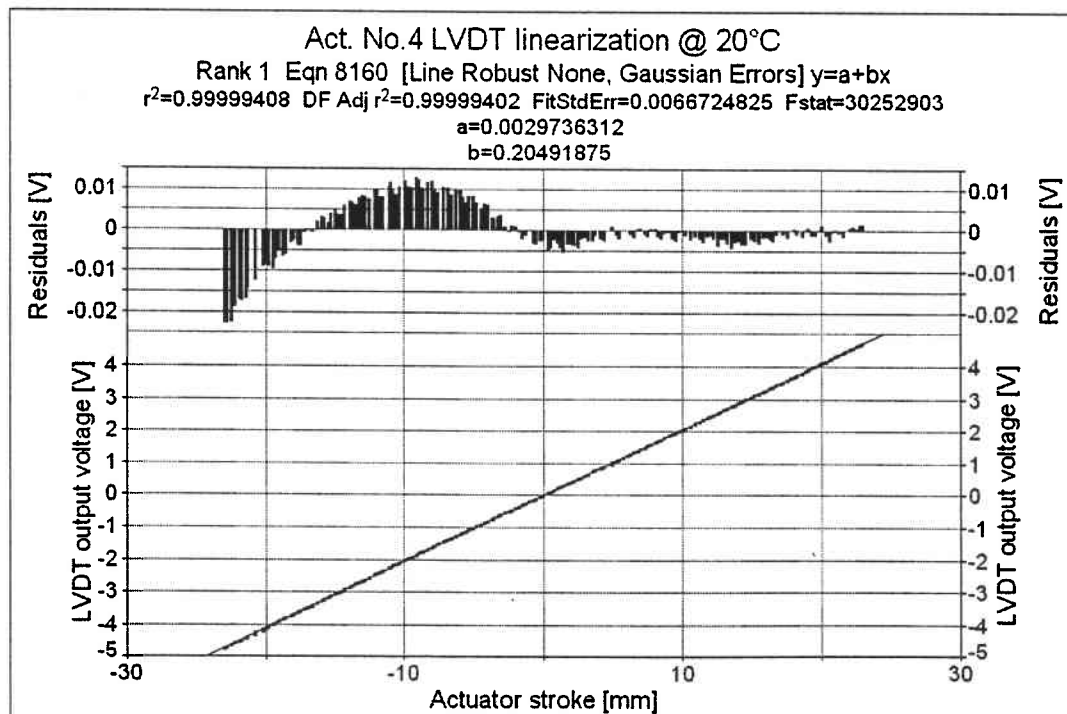


Figure 12 – Actuator #4 LVDT calibration curve.

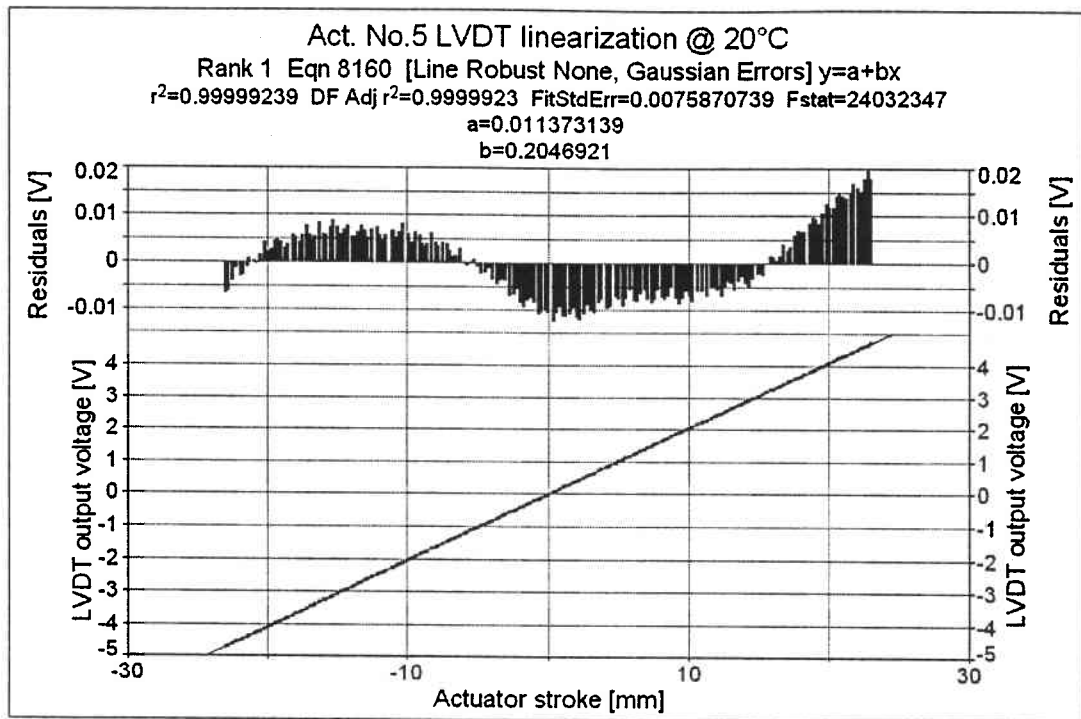
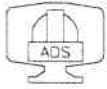


Figure 13 – Actuator #5 LVDT calibration curve.

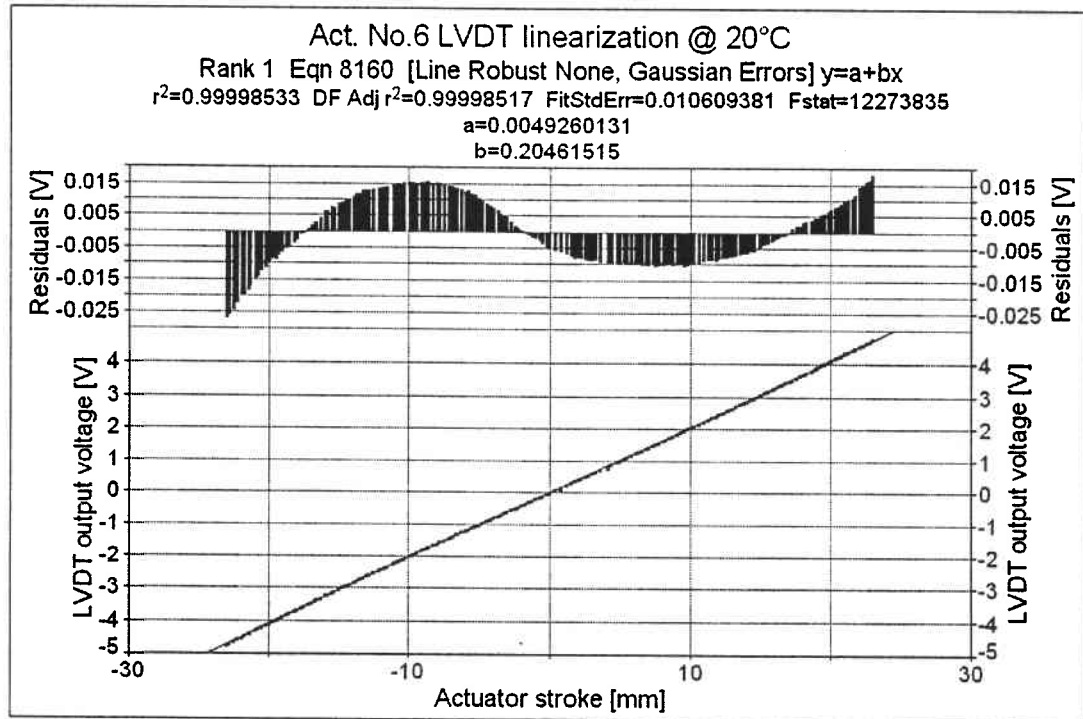


Figure 14 – Actuator #6 LVDT calibration curve.

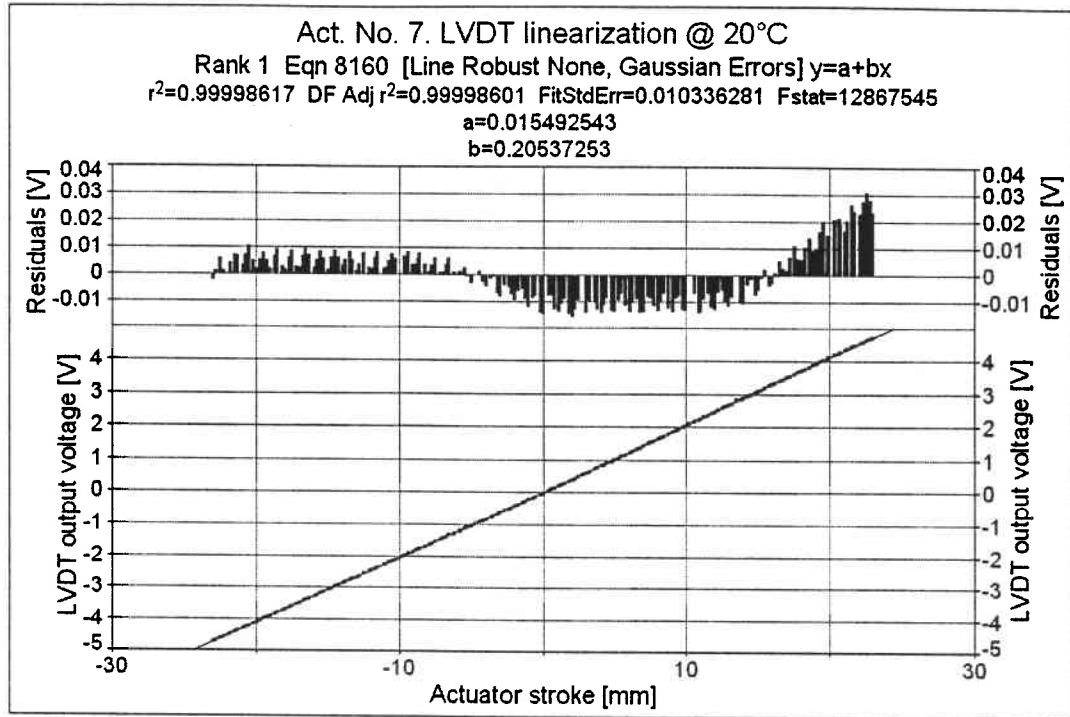


Figure 15 – Actuator #7 LVDT calibration curve.

Act.	1	2	3	4	5	6	7
Sens [V/mm]	0.20537	0.20469	0.20492	0.20521	0.20678	0.20461	0.20537
STD [mV]	16.95	7.58	6.67	6.61	3.24	10.61	10.33

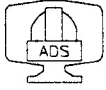
Table 4 – LVDT calibration values: summary of the measured values over all the seven actuators.

As a general result, it has been registered up to 25 mV deviation from the linearity which means about 122 μm in positioning error.

The non-linearities that have been plotted are very well repeatable, but it seems hard to compensate for more than 90% of this effect. If an absolute error of +/- 15 μm can be accepted over the entire 2" stroke, the LVDT could be used as absolute sensor.

Anyway, due to the high noise level of the sensor itself (30 mV ripple factory declared), special care should be taken if using the sensor as direct position feedback sensor inside the control loop.

It seems advisable to use the sensor just as an external static reference to be heavily filtered and used to reach the final absolute position (for example during the homing procedure).



4.3 Screw lead error

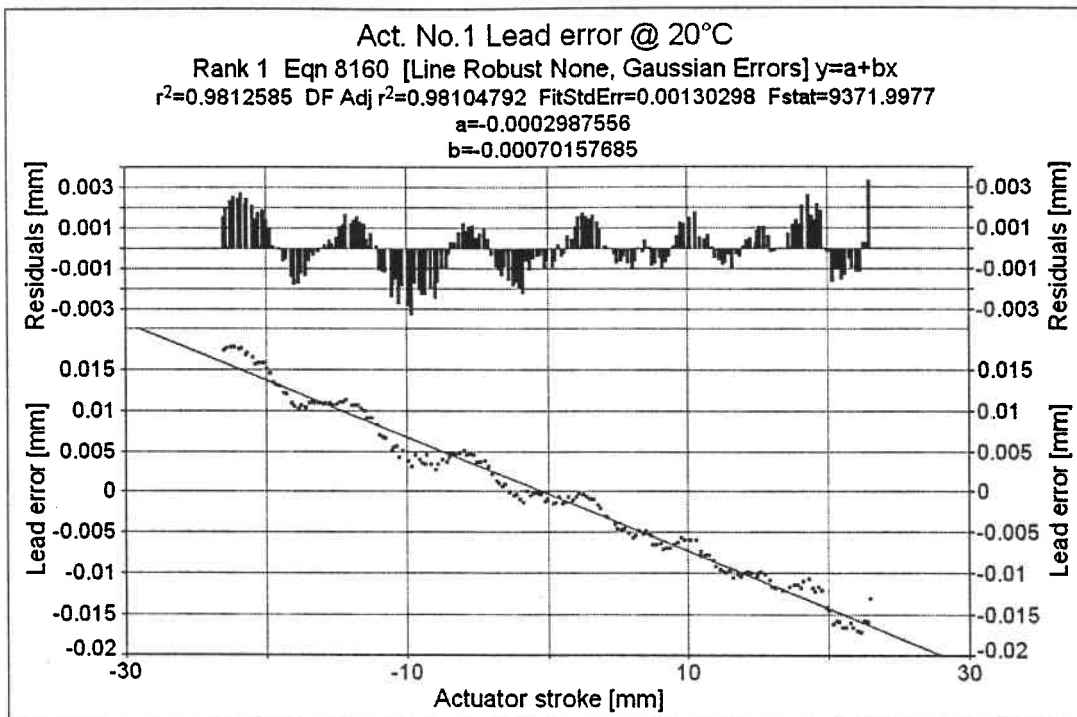


Figure 16 – Actuator #1 screw lead error.

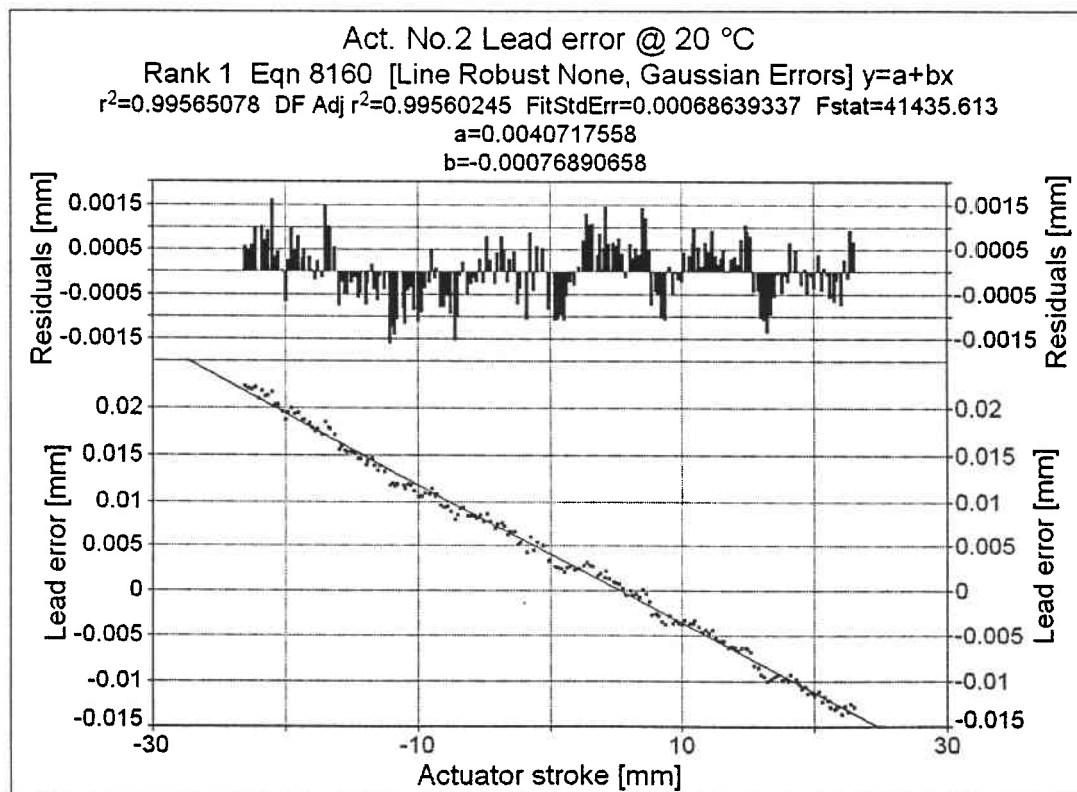


Figure 17 – Actuator #2 screw lead error.

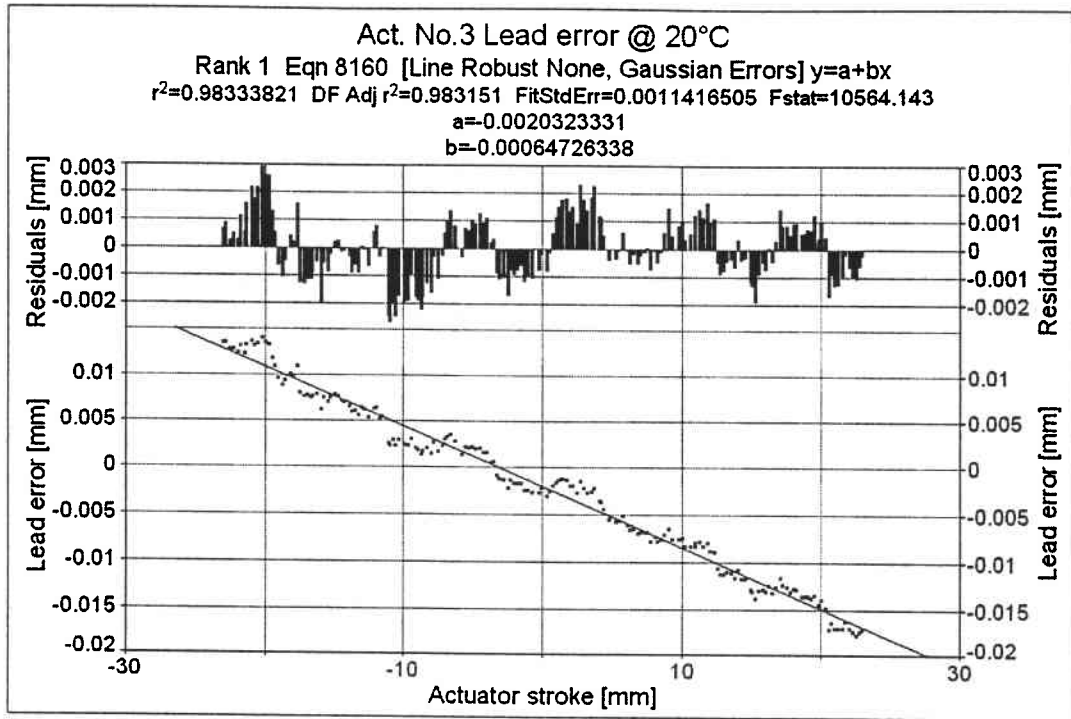


Figure 18 – Actuator #3 screw lead error.

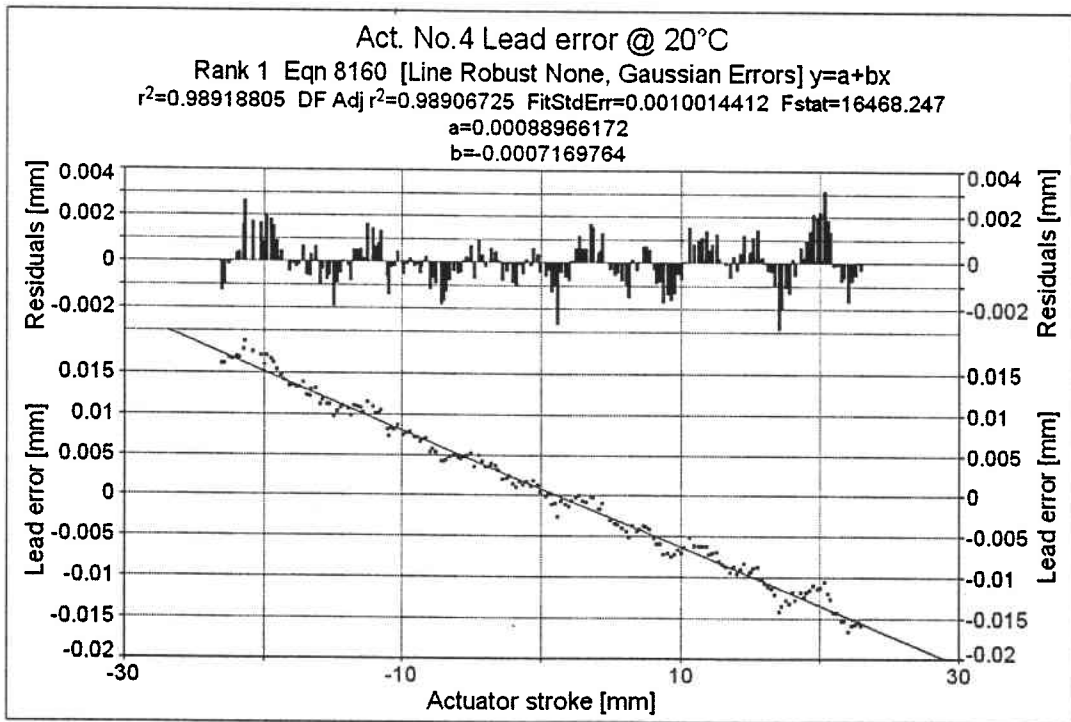


Figure 19 – Actuator #4 screw lead error.

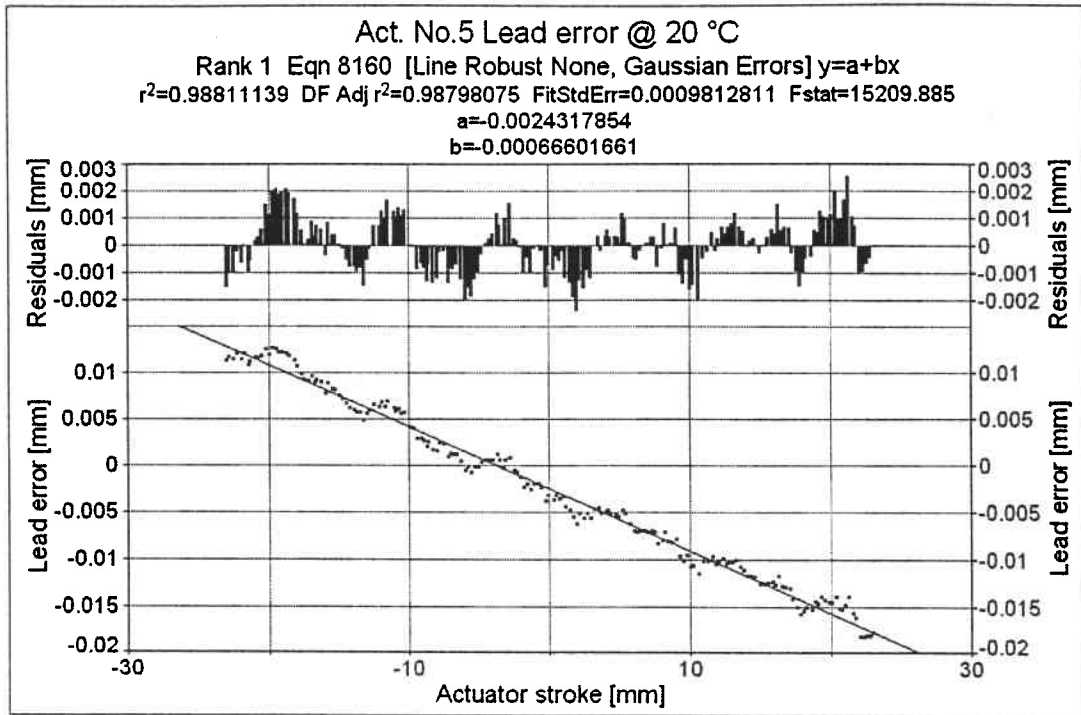
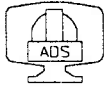


Figure 20 – Actuator #5 screw lead error.

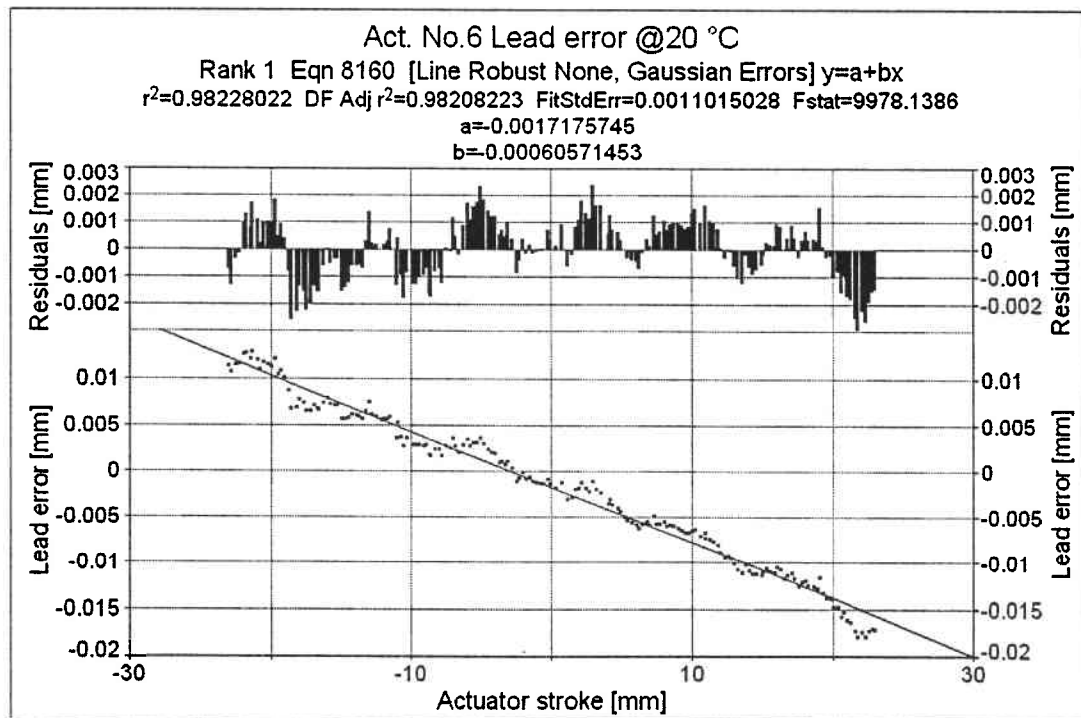


Figure 21 – Actuator #6 screw lead error.

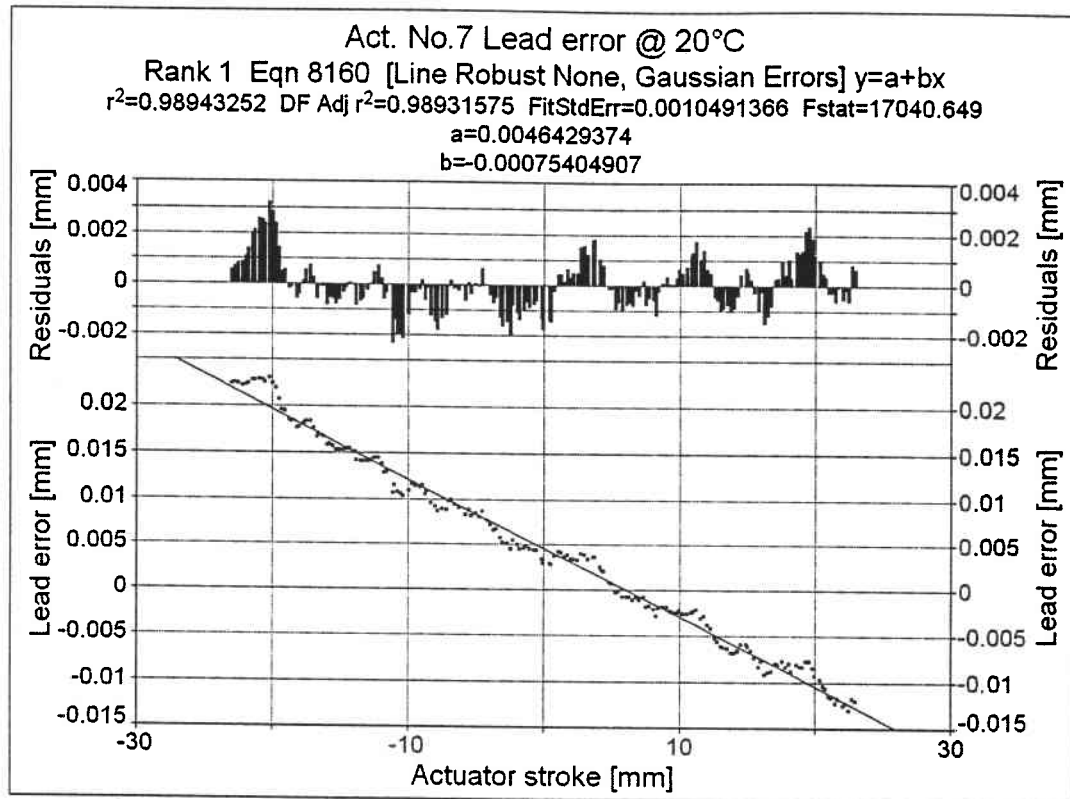
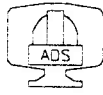


Figure 22 – Actuator #7 screw lead error.

Act. No.	1	2	3	4	5	6	7
L.e. [μm]	0.70	0.77	0.65	0.72	0.66	0.61	0.75
STD [μm]	1.3	0.7	1.1	1.0	1.0	1.1	1.0

Table 5 – The lead errors and the standard deviations from the linear behaviour are summarised for each actuator.

The lead error at ambient temperature is of the order of +/- 15 μm over the whole 46 mm stroke. To be noted that such error is comparable to the one that could be obtained from linearized LVDT.

Provided that the LVDT must be compensated also for the temperature drifts, the same thermal correction could also reduce the screw lead error to the STD level reported in table 5.

Therefore, these tests definitely suggest closing the position loop on the rotary encoder only while keeping the LVDT signal for absolute off-line reference and homing.



4.4 Repeatability

The following tables report the results of the repeatability tests as it was measured at different position along each actuator stroke.

Stroke [mm]	5	10	15	20	25	30	35	40	Average
PTV [μm]	1,2	0,6	0,8	0,5	1,0	1,1	1,3	1,9	1,05
STD [μm]	0,5	0,2	0,3	0,2	0,4	0,4	0,5	0,7	0,4

Table 6 – Actuator #1 repeatability test results.

Stroke [mm]	5	10	15	20	25	30	35	40	Average
PTV [μm]	0,8	0,4	1,0	0,6	0,5	0,4	0,5	1,2	0,68
STD [μm]	0,3	0,2	0,3	0,3	0,3	0,2	0,2	0,5	0,29

Table 7 – Actuator #2 repeatability test results.

Stroke [mm]	5	10	15	20	25	30	35	40	Average
PTV [μm]	0,3	0,9	0,8	0,5	1,7	0,9	1,6	1,0	0,96
STD [μm]	0,1	0,3	0,3	0,2	0,6	0,3	0,7	0,4	0,36

Table 8 – Actuator #3 repeatability test results.

Stroke [mm]	5	10	15	20	25	30	35	40	Average
PTV [μm]	1,4	0,9	0,5	0,3	0,6	1,0	0,3	1,2	0,78
STD [μm]	0,5	0,4	0,2	0,1	0,2	0,4	0,1	0,5	0,3

Table 9 – Actuator #4 repeatability test results.

Stroke [mm]	5	10	15	20	25	30	35	40	Average
PTV [μm]	0,6	0,2	0,7	0,7	-	-	-	-	
STD [μm]	0,2	0,1	0,3	0,3	-	-	-	-	

Table 10 – Actuator #5 repeatability test results.

Stroke [mm]	5	10	15	20	25	30	35	40	Average
PTV [μm]	0,5	1,0	0,8	1,3	0,7	1,4	0,6	0,6	0,86
STD [μm]	0,2	0,5	0,3	0,5	0,3	0,5	0,2	0,2	0,43

Table 11 – Actuator #6 repeatability test results.

Stroke [mm]	5	10	15	20	25	30	35	40	Average
PTV [μm]	0,3	0,6	0,5	0,5	0,9	0,6	1,2	1,7	0,79
STD [μm]	0,1	0,3	0,2	0,2	0,3	0,3	0,5	0,6	0,31

Table 12 – Actuator #7 repeatability test results.

4.5 Resolution

Tables 13..19 report the results of the resolution tests for the seven actuators. It is important to underline that all the commanded rotational counts are actually performed by the actuator, even for the 1 μm command (1 μm =14.4 cts). This means that the hardware is capable of easily resolving 1 μm steps.

Cmd. step [μm]	5	4	3	2	1	Max error
Reading [μm]	5.0	4.4	3.5	2.1	1.0	-
Error [μm]	0.0	0.6	0.5	0.1	0	0.6

Table 13 – Actuator #1 resolution test results.

Cmd. step [μm]	5	4	3	2	1	Max error
Reading [μm]	5.0	4.1	3.1	1.9	0.8	-
Error [μm]	0	0.1	0.1	-0.1	-0.2	0.2

Table 14 – Actuator #2 resolution test results.

Cmd. step [μm]	5	4	3	2	1	Max error
Reading [μm]	4.6	4.3	3.5	2.3	1.1	-
Error [μm]	-0.4	0.3	0.5	0.3	0.1	0.5

Table 15 – Actuator #3 resolution test results.

Cmd. step [μm]	5	4	3	2	1	Max error
Reading [μm]	5.1	4.4	3.5	2.2	0.9	-
Error [μm]	0.1	0.4	0.5	0.2	-0.1	0.5

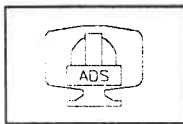
Table 16 – Actuator #4 resolution test results.

Cmd. step [μm]	5	4	3	2	1	Max error
Reading [μm]	5.1	4.1	3.0	2.3	0.8	-
Error [μm]	0.1	0.1	0.0	0.3	-0.2	0.3

Table 17 – Actuator #5 resolution test results.

Cmd. step [μm]	5	4	3	2	1	Max error
Reading [μm]	5.3	4.4	3.7	2.3	0.9	-
Error [μm]	0.3	0.4	0.7	0.3	-0.1	0.7

Table 18 – Actuator #6 resolution test results.



Cmd. step [μm]	5	4	3	2	1	Max error
Reading [μm]	4.6	3.9	3.0	1.9	0.5	-
Error [μm]	-0.4	-0.1	0.0	-0.1	-0.5	0.4

Table 19 – Actuator #7 resolution test results.

Act. #	1	2	3	4	5	6	7
SDE [μm]	0.6	0.2	0.5	0.5	0.3	0.7	0.4

Table 20 – Small Displacement Errors: for each actuator it is reported the largest error measured for all the steps performed.

As can be seen, the sub-micron level of the error is absolutely acceptable considering the external linear reference intrinsic limitation due to its mount on the guiding unit. In fact, the difference between the displacement read by the linear encoder on the bench and the rotary one can be due not only to actuator’s imperfections but also to the test bench deformation.

4.6 Backlash

In the frame of this test the LVDT electrical noise was measured as well. The test is reported in table 21 where the averaged LVDT output is reported for a fixed position of the actuator.

LVDT counts	Decimal	LVDT counts	Decimal	LVDT counts	Decimal
32778,165	0,165	32778,183	0,183	32778,225	0,225
32778,144	0,144	32778,222	0,222	32778,183	0,183
32778,136	0,136	32778,19	0,190	32778,15	0,150
32778,093	0,093	32778,147	0,147	32778,195	0,195
32778,113	0,113	32778,19	0,190	32778,242	0,242
32778,121	0,121	32778,203	0,203		
32778,126	0,126	32778,229	0,229	Average [cts]	0,17183
32778,148	0,148	32778,202	0,202	STD [cts]	0,00160
32778,18	0,180	32778,165	0,165	PTV [cts]	0,14900

Table 21 – LVDT filtered output for still actuator (brake on): the samples were taken at 2 kHz and the each measure is the average of 2000 samples.

The standard deviation of the digitally filtered signal is about 0.003 μm that is well below the range of interests. Also the PTV variation among the averaged readings (0.149 cts = 0.22 μm) is well acceptable for this kind of investigation.

This means that the LVDT provides a sufficient stability of the signal from the electrical point of view, provided the proper digital filtering is implemented.

Hereafter the results of act. No. 6 are detailed reported in order to show the test procedure. For the other actuators only the residual backlash is then reported.

$\mu\text{m}_{\text{SCREW}}$	Heidenhain [mm]	LVDT counts	
22000	0.0000	47576.93	
22100	0.1003	47646.87	
22000	0.0063	47577.36	$\Delta_{\text{LVDT}} = 0.43 \text{ cts} = 0.64 \mu\text{m}$
22000	0.0000	47576.45	
22100	0.1001	47646.12	
22000	0.0050	47576.92	$\Delta_{\text{LVDT}} = 0.47 = 0.70 \mu\text{m}$

Table 22 – Actuator #6: backlash measurement sequence at extended position.

$\mu\text{m}_{\text{SCREW}}$	Heidenhain [mm]	LVDT counts	
0	0.0000	32771.25	
100	0.0979	32838.26	
0	0.0010	32771.33	$\Delta_{\text{LVDT}} = 0.08 \text{ cts} = 0.11 \mu\text{m}$
0	0.0000	32771.43	
100	0.0985	32838.51	
0	0.0006	32771.51	$\Delta_{\text{LVDT}} = 0.08 \text{ cts} = 0.11 \mu\text{m}$

Table 23 – Actuator #6: backlash measurement sequence at midstroke position.

$\mu\text{m}_{\text{SCREW}}$	Heidenhain [mm]	LVDT counts	
-22000	0.0000	17952.28	
-22100	0.1001	17883.22	
-22000	0.0050	17952.14	$\Delta_{\text{LVDT}} = 0.14 \text{ cts} = 0.2 \mu\text{m}$
-22000	0.0000	17952.08	
-22100	0.0993	17882.43	
-22000	0.0023	17951.99	$\Delta_{\text{LVDT}} = 0.09 \text{ cts} = 0.14 \mu\text{m}$

Table 24 – Actuator #6: backlash measurement sequence at closed position.

Test	Back. Heidenhain [μm]	Back. LVDT [cts]	Back LVDT [μm]
Extd. 1	2,6	0,702	1,04
Extd. 2	2,5	0,555	0,83
Center 1	1,9	0,907	1,35
Center 2	1,7	0,170	0,25
Closed 1	2,3	1,970	2,93
Closed 2	2,9	1,730	2,57
Average	2,32	1,006	1,5

Table 25 – Actuator #1: backlash measurement results.



MMT CONVERSION
M2 f/5 HEXAPOD

Doc.No: H5-TR-AD-01001

Issue : A

Date : 21 April 2001



Test	Back. Heidenhain [μm]	Back. LVDT [cts]	Back LVDT [μm]
Extd. 1	3,5	0,132	0,196
Extd. 2	3,5	0,564	0,840
Center 1	2,4	0,161	0,239
Center 2	2,5	0,056	0,084
Closed 1	1,3	0,256	0,382
Closed 2	1,5	0,241	0,359
Average	2,45	0,235	0,35

Table 26 – Actuator #2: backlash measurement results.

Test	Back. Heidenhain [μm]	Back. LVDT [cts]	Back LVDT [μm]
Extd. 1	5,1	0,262	0,39
Extd. 2	5,0	0,903	1,34
Center 1	3,7	0,349	0,52
Center 2	3,4	0,602	0,89
Closed 1	1,3	0,151	0,22
Closed 2	1,3	0,240	0,36
Average	3,3	0,418	0,62

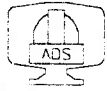
Table 27 – Actuator #3: backlash measurement results.

Test	Back. Heidenhain [μm]	Back. LVDT [cts]	Back LVDT [μm]
Extd. 1	5,1	1,503	2,23
Extd. 2	5,9	1,734	2,58
Center 1	2,0	0,132	0,19
Center 2	2,1	0,074	1,10
Closed 1	2,2	0,364	0,54
Closed 2	3,5	1,036	1,54
Average	3,47	0,807	1,36

Table 28 – Actuator #4: backlash measurement results.

Test	Back. Heidenhain [μm]	Back. LVDT [cts]	Back LVDT [μm]
Extd. 1	6,6	0,036	0,05
Extd. 2	6,0	0,500	0,74
Center 1	3,5	0,200	0,29
Center 2	3,8	0,531	0,79
Closed 1	6,1	1,183	1,76
Closed 2	5,3	1,490	2,22
Average	5,22	0,657	0,98

Table 29 – Actuator #5: backlash measurement results.



Test	Back. Heidenhain [μm]	Back. LVDT [cts]	Back LVDT [μm]
Extd. 1	6,3	0,43	0,64
Extd. 2	5,0	0,47	0,70
Center 1	1,0	0,08	0,11
Center 2	0,6	0,08	0,11
Closed 1	5,0	0,14	0,20
Closed 2	2,3	0,09	0,14
Average	3,37	0,22	0,32

Table 30 – Actuator #6: backlash measurement results.

Test	Back. Heidenhain [μm]	Back. LVDT [cts]	Back LVDT [μm]
Extd. 1	6,3	0,182	0,27
Extd. 2	7,2	0,575	0,85
Center 1	2,4	0,743	1,11
Center 2	2,7	1,096	1,63
Closed 1	0,7	0,178	0,26
Closed 2	0,9	0,027	0,04
Average	3,37	0,467	0,69

Table 31 – Actuator #7: backlash measurement results.

The average backlash of the actuators is always less than 1.5 μm .

It seems that the backlash average value is the most significant among the measured ones, because no evidence of clear dependence on the actuator position has been demonstrated.

Such phenomena can be due to the different screw-nut couplings that can happen as the actuator changes its position.

Moreover, the measurements of both the linear encoder and the LVDT can be affected by mechanical imperfections on the sliding unit that holds the actuator



4.7 Step response

Figures 23..29 reports the plots of the seven actuators step responses.

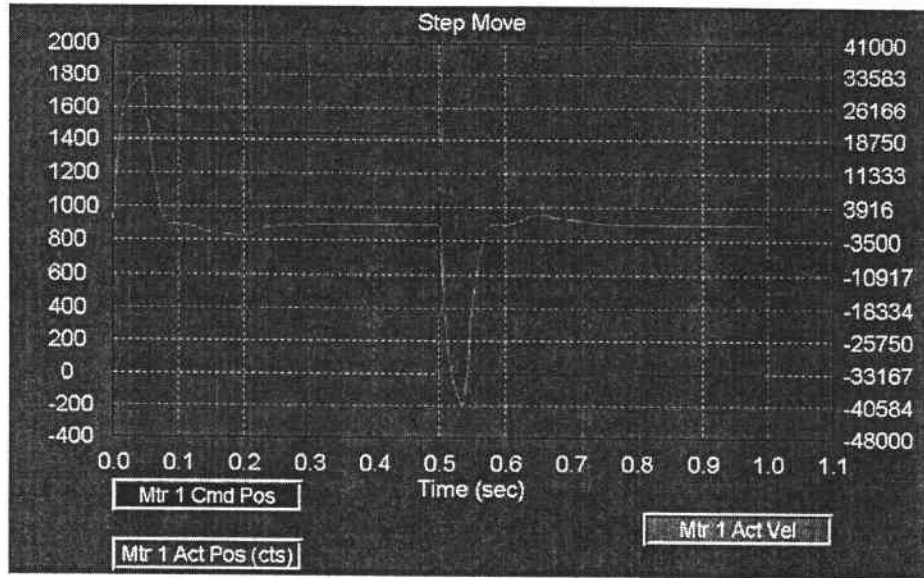


Figure 23 – Actuator #1 step response.

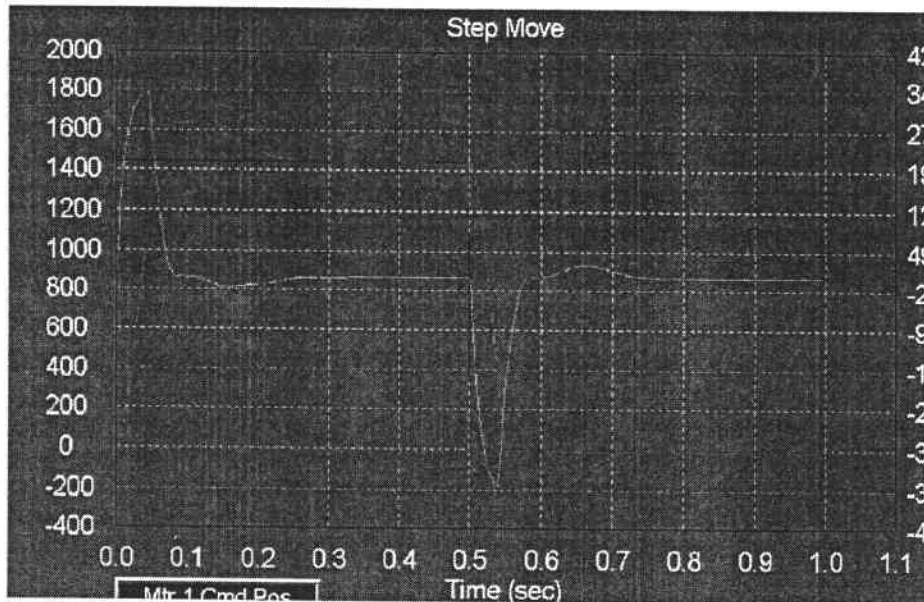


Figure 24 – Actuator #2 step response.

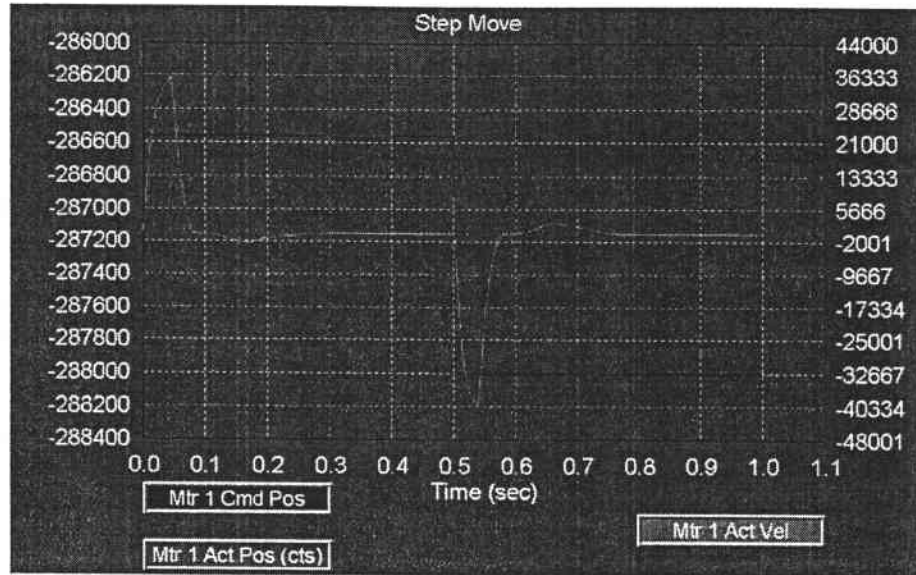


Figure 25 – Actuator #3 step response.

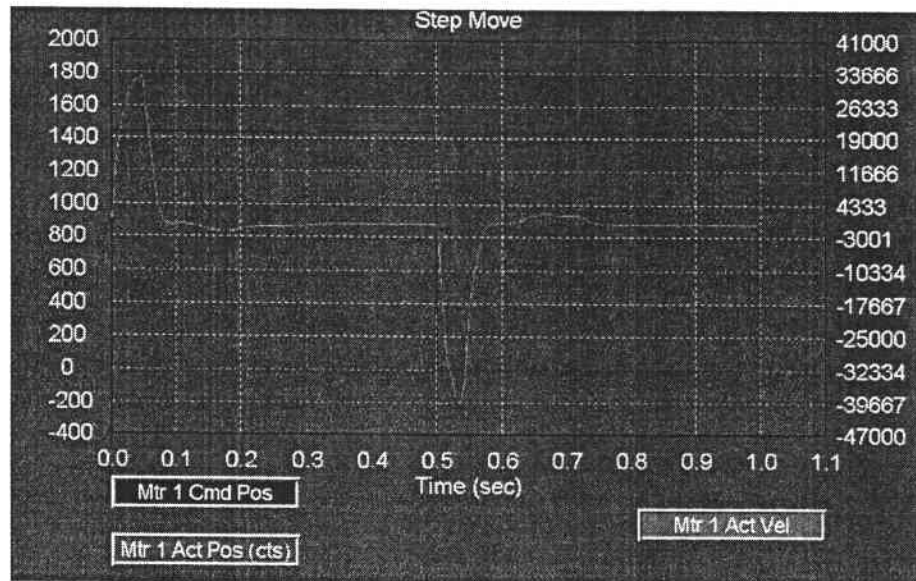


Figure 26 – Actuator #4 step response.

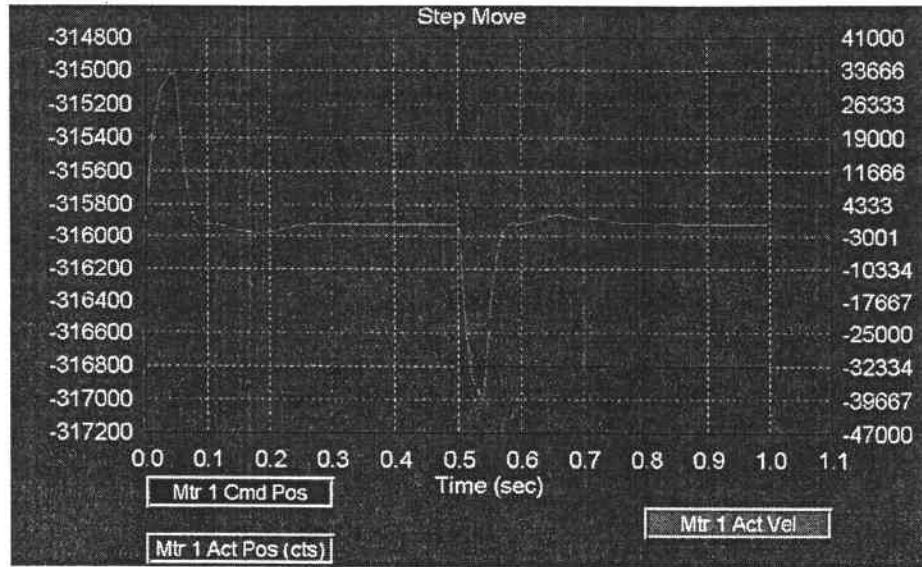


Figure 27 – Actuator #5 step response.

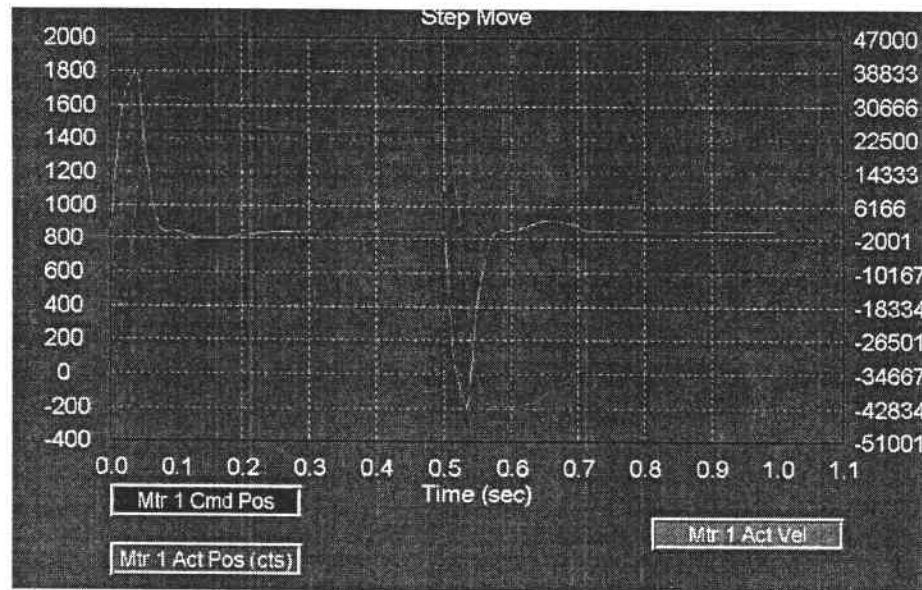


Figure 28 – Actuator #6 step response.

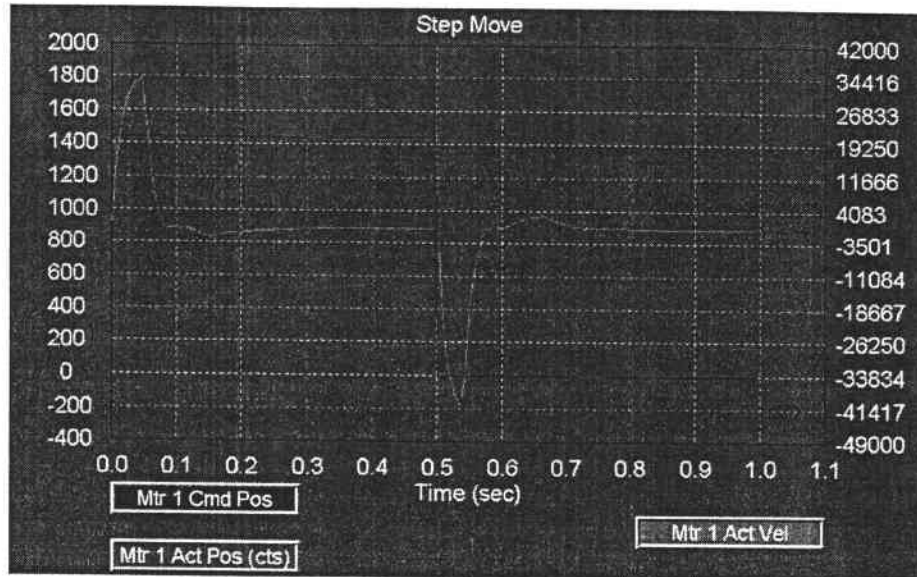
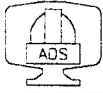


Figure 29 – Actuator #7 step response.

The final position is reached in about 0.3 seconds, with a peak speed equal to 38000 cts/seconds that corresponds to 2.63 mm/s.

In all cases, the speed specifications is largely achieved ($> 300 \mu\text{m/s}$).

4.8 Power consumption

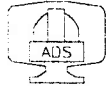
The results of the power consumption tests are reported in the following tables.

Extra load [N]	Current _{CRUISE} [A]	W _{CRUISE} [W]
0	1.68	28.5
867	1.95	33.1
Power _{CRUISE} [W] = 28.5+ 5.3 x10 ⁻³ x Newton		

Table 32 – Actuator #1: power consumption results.

Extra load [N]	Current _{CRUISE} [A]	W _{CRUISE} [W]
0	1.61	27.3
630	1.81	30.7
Power _{CRUISE} [W] = 27.3 + 5.3 x10 ⁻³ x Newton		

Table 33 – Actuator #2: power consumption results.



Extra load [N]	Current _{CRUISE} [A]	W _{CRUISE} [W]
0	1.65	28.1
760	1.88	31.9
Power _{CRUISE} [W] = 28.1 + 5.0 x 10 ⁻³ x Newton		

Table 34 – Actuator #3: power consumption results.

Extra load [N]	Current _{CRUISE} [A]	W _{CRUISE} [W]
0	1.85	31.4
735	2.05	34.8
Power _{CRUISE} [W] = 31.4 + 4.6 x 10 ⁻³ x Newton		

Table 35 – Actuator #4: power consumption results.

Extra load [N]	Current _{CRUISE} [A]	W _{CRUISE} [W]
0	1.80	30.6
867	2.04	34.6
Power _{CRUISE} [W] = 30.6 + 4.6 x 10 ⁻³ x Newton		

Table 36 – Actuator #5: power consumption results.

Extra load [N]	Current _{CRUISE} [A]	W _{CRUISE} [W]
0	1.65	28.5
759	1.88	31.9
Power _{CRUISE} [W] = 28.5 + 4.5 x 10 ⁻³ x Newton		

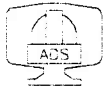
Table 37 – Actuator #6: power consumption results.

Extra load [N]	Current _{CRUISE} [A]	W _{CRUISE} [W]
0	1.60	27.2
759	1.85	31.4
Power _{CRUISE} [W] = 27.2 + 5.6 x 10 ⁻³ x Newton		

Table 38 – Actuator #7: power consumption results.

By taking the average behaviour of all the actuators, the power consumption as function of the applied actuator axial load is:

$$\text{Power}_{\text{CRUISE}} [\text{W}] = 28.8 + 5.0 \times 10^{-3} \times \text{Newton}$$



5. HP TESTS

Three parameters have been measured on the hexapod once it has been integrated: the weight, the distance between the plates and the axial stiffness.

5.1 Weight

The mass of the hexapod has been measured being 146 Kg, with a load cell accuracy of 2 Kg.

5.2 Distance between the plates

The height of the upper plate has been measured by a electronic multi-axis milling machine, with a contact probe replacing the working head.

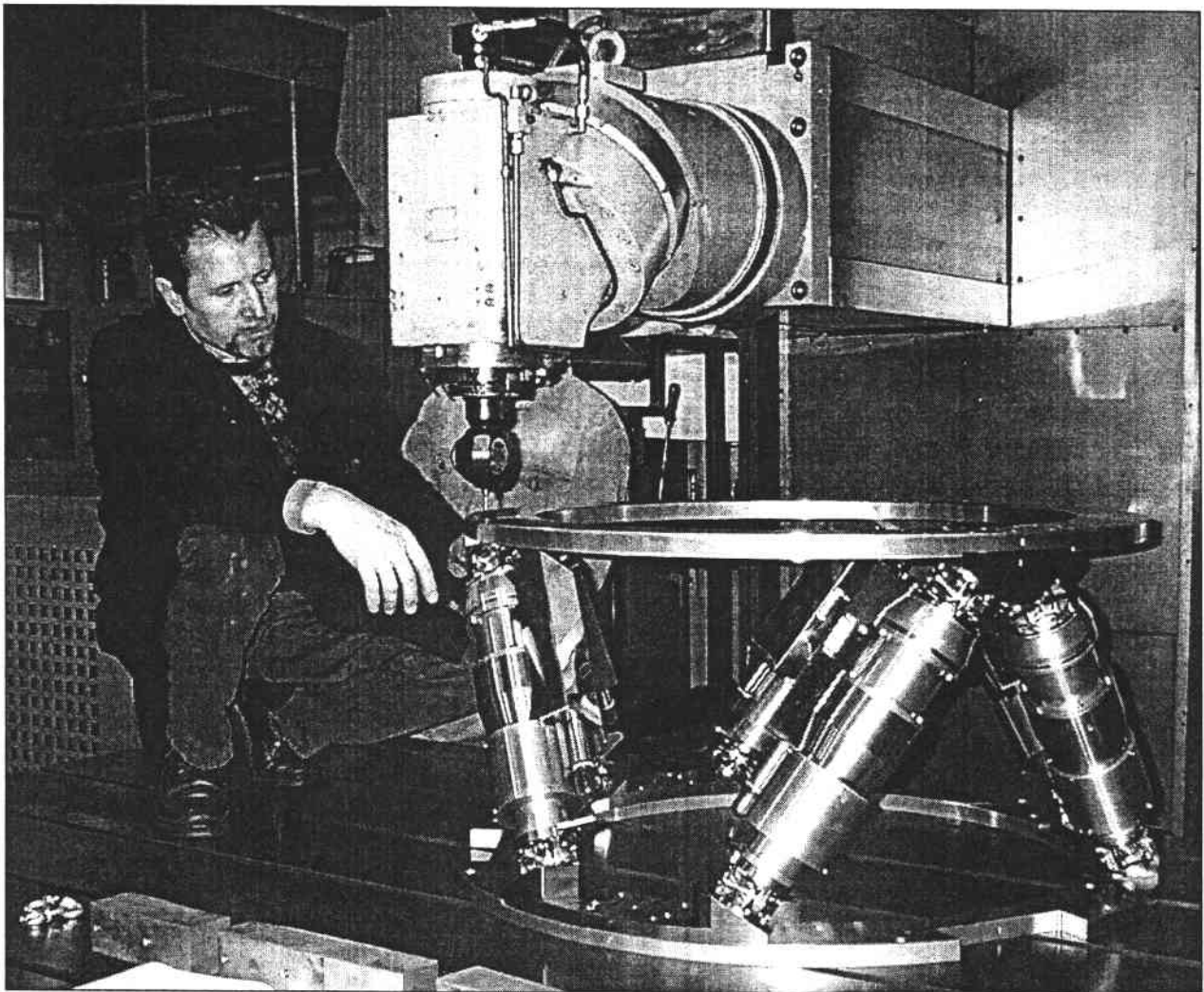
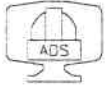


Figure 30 – The geometrical test on the assembled hexapod.



The planarity of the machine bench where the hexapod was placed has been measured being 0.03 mm/m.

The reading of the machine was reset by touching the upper plate over the wedge #1. The height measured over the wedges #2 and #3 was 0.31 mm and 0.35 mm respectively.

A final check of the height of point #1 after the measurement showed an error of 0.05 mm.

Based on this result, the PTV of the upper plate height with respect to the mobile plate can be estimated being 0.30 mm.

This measure defines the shape of the hexapod referred to the current null reading of the actuators LVDTs.

5.3 Axial stiffness

A compression load sequence was applied to the hexapod.

A steel plate was put on the upper flange through three spacers that allowed introducing the load on the three wedges. Three gauges were placed on the bench touching the upper flange under the three wedges.

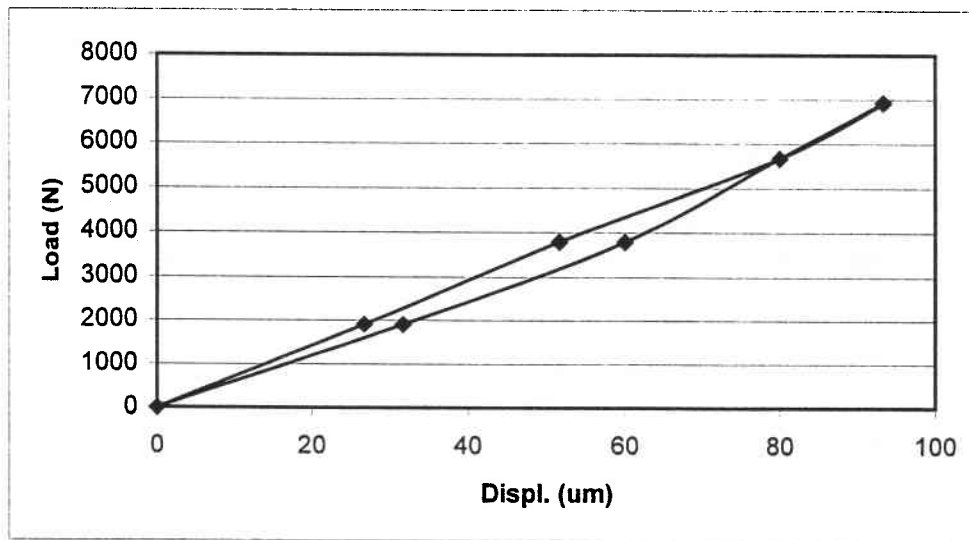


Figure 31 – The axial stiffness test of the assembled hexapod.

The resulting axial stiffness of the hexapod is 74 N/ μ m.

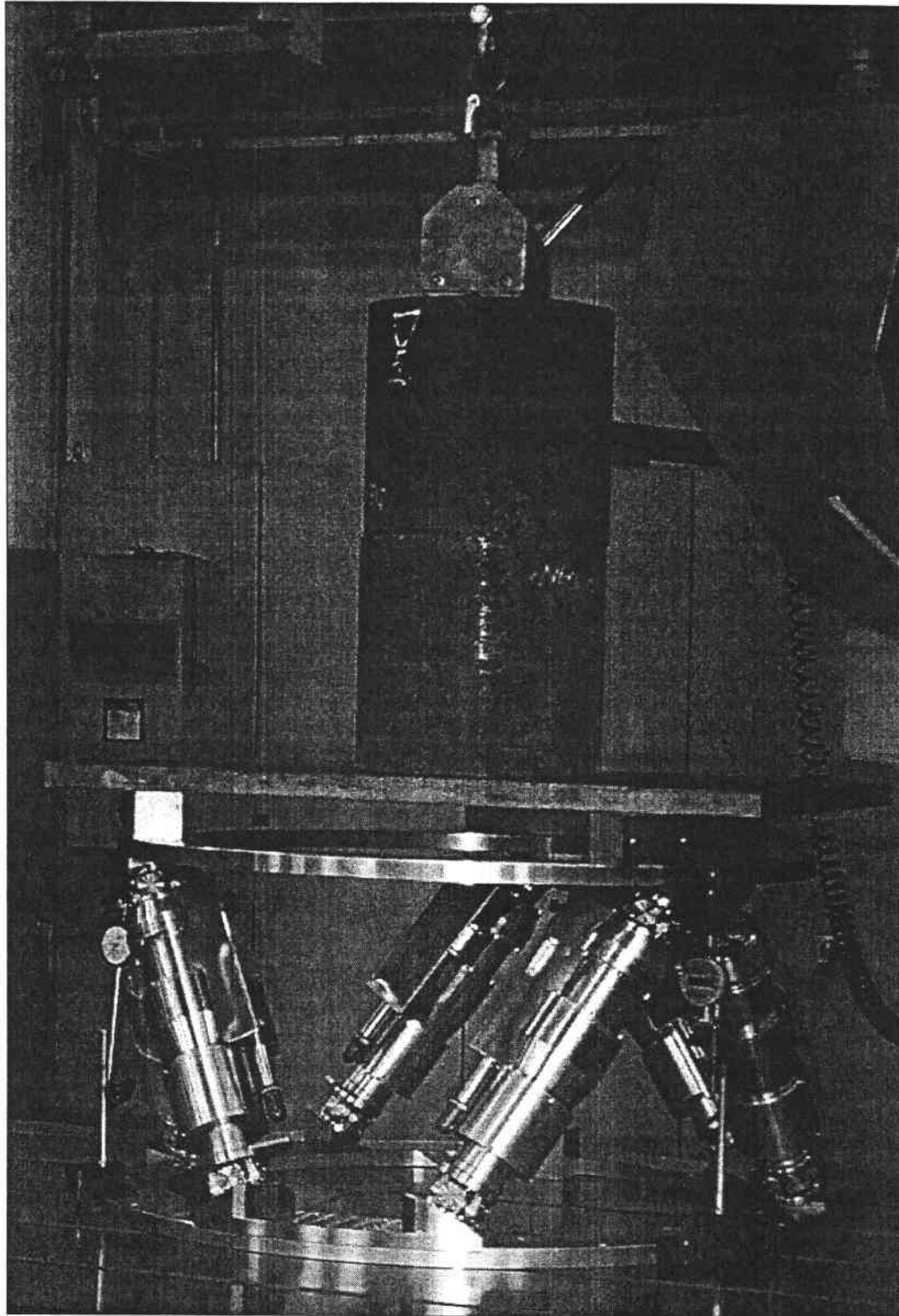
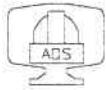


Figure 32 – The axial stiffness test of the assembled hexapod.



6. FINAL REMARKS

All the seven linear actuators of the MMT M2 f/5 hexapod have been tested and aligned.

Some tests results were systematically affected by the limitations of the test bench, especially for what concerns the stiffness of the linear guide and the trolley that mount the mobile end of the actuator.

The axial stiffness test performed on the entire hexapod gave a result of 74 N/ μ m. By comparing such measure with the numerical model one can derive an average value of 20 N/ μ m for the actuators axial stiffness. The difference with respect to the individual actuators test results can be due both to a poor measurement of the test bench own stiffness and to the low level of the applied loads.

The repeatability test results showed a micron level repeatability over all the actuators (worst case 1.05 μ m error).

The measured backlash on all the actuators stays below 1.5 μ m.

The step response test showed the full achievement of the speed specifications.

Finally, the power absorption tests indicate that each actuator takes 5 mWatt/Newton plus about 30 Watt for the driver.

ADS International S.r.l.

Legal Office: via Clerici, 14 I-20032 – Cormano (Mi) – Italy
Technical and administrative office: c.so Promessi Sposi, 23/d I-23900 – Lecco – Italy
VAT # 12279020155 – R.I. Milano 16547/1998 – REA Milano 1546550 – REA Lecco 287107
Contacts. Phone: +390341259231 – Fax: +390341259235 – URL: www.ads-int.com